Design, Construction, and Evaluation of an RC Vehicle Dynamometer

by
Christian Marron

BioResource and Agricultural Engineering

BioResource and Agricultural Engineering Department

California Polytechnic State University

San Luis Obispo

2014

TITLE : Design, Construction, and Evaluation of an RC Vehicle Dynamometer

AUTHOR : Christian Marron

DATE SUBMITTED : June 6, 2014

Dr. Mark Zohns

Senior Project Advisor

Signature

6-6-14

Date

Dr. Art MacCarley

Department Head

Signature

4/2/15

Date

ACKNOWLEDGEMENTS

I would first like to recognize the excellent faculty guidance and assistance throughout the course of this project. First, my project advisor, Dr. Mark Zohns has been a tremendous influence both on my project, as well as my entire college career, in providing me with the skills and enthusiasm to understand and analyze mechanical systems.

Additionally, I would like to thank Mr. Virgil Threlkel for his immense patience and aid in teaching me the basics of machining operations. Mr. Threlkel has taught me virtually all of the hands on skills required to machine and fabricate devices of any caliber. These skills and techniques I have acquired under his supervision have reinforced the BioResource and Agricultural Engineer Department motto, **"life-long learning."**

I would also like to thank my parents, Lydia and Michael Marron, for all of the support they have provided me with to get through the rigorous BioResource and Agricultural Engineering program here at Cal Poly.

Lastly, I would like to thank Mr. Ken Crane for producing the SimpleDyno software that was used to analyze the performance of various vehicles.

ABSTRACT

This senior project report contains the design, construction, and testing of an RC Vehicle Dynamometer. Various design factors for an inertial based dynamometer are discussed and analyzed in depth to produce the most appropriate final product.

The dynamometer utilizes a software program, SimpleDyno, as the data acquisition system to measure and quantify the performance of various RC vehicles. A series of tests using the dynamometer were then conducted to measure the speed, torque, and horsepower produced by the different vehicles.

DISCLAIMER STATEMENT

The university clearly states that the information forwarded regarding this project is a direct result of a class assignment and has been graded and accepted only as a fulfillment of a course requirement. Acceptance by the university does not imply technical accuracy or reliability. Any use of the information in this report is made by the user(s) at his or her own risk, which may include failure of the device or infringement of patent or copyright laws. Therefore, the recipient and/or user of the information contained in this report agrees to indemnify, defend and save harmless the State its officers, agents and employees from any and all claims and losses accruing or result to any person, form, or corporation who may be injured or damaged as a result of the use of this report.

TABLE OF CONTENTS

LIST OF FIGURES

Page

LIST OF TABLES

Page

INTRODUCTION

The need for increased performance and power in race vehicles is an ongoing cycle that has no end in sight. Whether the vehicle ranges from Formula-1 race spec teams to hobby enthusiasts, the demand for excellence is always pressing. Dynamometers are an essential tool in measuring a vehicle's performance prior to on-road track testing to ensure maximum performance of the vehicle. By utilizing this tool, vehicle components may be fine-tuned so that an initial vehicle performance level may be set.

Just like any race spec vehicles, radio controlled, or R/C, vehicles require the same level of fine tuning and testing to achieve maximum performance. The R/C industry has been growing exponentially since the releases of the first R/C vehicles in the 60's and the vehicles have been evolving ever since. This steady growth has led to the development of the Remotely Operated Auto Racers (ROAR) foundation which now organizes professional R/C races in both the United States and Canada. The establishment of the ROAR foundation has brought forth the emergence of many professional racers who have dedicated their life to the hobby. Unfortunately, many of these racers and enthusiasts are limited to testing their vehicles entirely on the track and evaluate their modifications and tuning entirely "by feel." As a result, this has presented the opportunity of developing an R/C vehicle dynamometer to evaluate the performance of these race level vehicles. By utilizing a dynamometer, individuals will now be able to visibly see and now quantify how their adjustments affect the performance of their vehicles.

The project objective is to design and fabricate an inertia based chassis dynamometer to test R/C vehicles. In order to successfully accomplish this, the main focus of the dynamometer is adjustability. This is due to the varying wheel bases and overall class scale differences between the vehicles. Thus, it will be necessary to have an adjustable roller wheel base so that the dynamometer will accommodate various scale vehicle classes. The difference in scale will also lead to a deviation in vehicle weight; therefore the prime rollers that will be adequate for various class scales. Lastly, the dynamometer will require adjustable safety restraints and rear media shields to restrain the vehicle and shield from projectiles lodged in the tires.

This completed dynamometer must be within a $200-$300 price range so that the recreation of this dynamometer will be feasible and economical. While price governs a significant portion of the design, the final dynamometer must also be light and portable so that it may be used between race events at track sites. In order to accumulate and record the results of testing, the SimpleDyno software will be used in conjunction with a laptop. This will allow for universal testing on any computer or laptop and access for any individual interested in replicating the design.

LITERATURE REVIEW

This portion of the report is intended to provide the reader with information regarding the key components and important aspects regarding chassis' dynamometers.

Dynamometer Functionality

A chassis dynamometer is a device that is commonly used to measure the torque and power output that is delivered to the wheels of a vehicle (DTEC 2002). The chassis dynamometer records the speed of the vehicle's wheels as the vehicle's power system is engaged. Using a series of free rollers, between two and four rollers in total, the chassis dynamometer allows the vehicle's wheels to rotate freely on the rollers, while safely securing it to the dynamometer frame. Figure 1 below demonstrates the basic application of the chassis dynamometer.

Figure 1. Basic Chassis Dynamometer.

Types of Dynamometers

There are a number of different types of dynamometers that are available to measure the vehicles output power. It is important to note the two main types of dynamometers used in the automotive industry, the chassis dynamometer and the engine dynamometer. The chassis dynamometer is used to measure the torque and power output through the drive train to the wheels of the vehicle without removing the power source from the vehicle. An engine dynamometer is coupled directly to output shaft of the motor or engine by removing it from the vehicle (DTEC 2002).

The chassis dynamometer may be further categorized depending on the dynamometer's method of testing. There are many types of chassis dynamometers, including the mechanical friction brake system, hydraulic or water brake system, electric variable system, and inertial based system (Garcia 2012). Most of the dynamometers above may be classified as either an absorption unit or an active unit. An absorption unit is designed to be driven by the vehicles wheels and act as a load, while an active unit may both drive

and absorb (EE 2014). It is important to note that inertial dynamometers are not to be confused with absorption units because they do not induce a load onto the vehicle. Rather they are intended to calculate power solely by measuring the power required to accelerate a known mass of the roller and provide no variable load to the prime mover (EE 2014).

The mechanical friction brake chassis dynamometer utilizes an induced load on the rollers of the dynamometer. The induced load may be used to calculate the torque generated by the motor or engine while the engine RPM is typically measured using a tachometer (L&SDCDS 2014). Through this process brake horsepower may be easily calculated and the measured torque is considered to be the most accurate reading.

The hydraulic-brake system utilizes a similar technique as the mechanical brake system to measure the torque and output power of the motor; however, there are no mechanical applications, only fluid hydraulics (Garcia 2012). A pump and reservoir are linked together so that fluid is pumped through the rollers and the valve is slowly closed once the engine has reached the desired RPM. This action creates a variable load on the engine, which allows for the calculation of both power and brake horsepower, by factoring a change in flow volume, pressure, and RPM.

The water-brake dynamometer is a system that induces a hydraulic load on the dynamometer's rollers. The water-brake system differs from that of the hydraulic-brake system because it uses water as the hydraulic fluid as opposed to oil. The water-brake system also allows for variable load on the rollers and has high power absorbance capabilities (Garcia 2012).

The electrical Eddy current absorption unit is a system that induces a resisting load through an AC or DC motor (Zhao 2012). These motors are typically equipped with a variable frequency drive, allowing for variable load on the rollers, which may be used to measure friction or pumping losses.

The inertial based chassis dynamometer is a system that utilizes a set of rollers as the parameters to conduct the testing. This type of dynamometer measures the acceleration of the roller with a known mass that is driven by the vehicle's wheels (DTEC 2002). Attached to the roller is a sensor that transfers the recorded data to either a data acquisition device or computer to reveal the results. In order for this system to be accurate and effective, the mass of the roller must be known in order to generate precise results and quantify the output of the vehicle using the following equations derived in the following section (Sadhukhan 2014).

Applicable Kinematics

The inertial based chassis dynamometer is based off of a series of kinematic equations, which allow for the calculation of desired outputs such as power and torque. These values will be dependent on the measured angular acceleration and computed inertia. The following equations are listed to provide the reader with an understanding of the derivation and the application of each variable.

$$\Theta = \frac{s}{r} \tag{1}$$

Equation 1 is used to determine the Angular Displacement (Θ) of a body. This displacement is calculated using the length of the arc traveled (s) divided by the radius of the circular path (r). By using this equation, one may determine the amount of rotation that has occurred within a body or in this case, the dynamometer's rollers. In Figure 2 below, one may observe how the angular displacement behaves within a body based on the parameters stated.

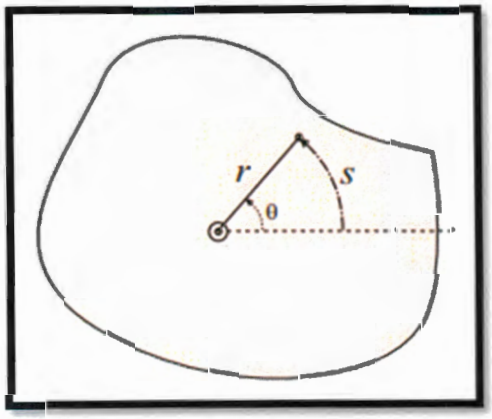

Figure 2. Rotation of an object about a fixed axis.

$$\omega = \frac{\Delta\theta}{\Delta t} \tag{2}$$

Equation 2 is used to determine the Angular Velocity (ω) of a body in motion. This angular velocity is calculated by dividing the total change in angular displacement (Θ) by the change in time (t). The angular velocity will play a key role in determining how fast the rollers are spinning due to the vehicle's tire rotation and the final power output of the vehicle's motor and power train system.

$$\alpha = \frac{\Delta\omega}{\Delta t} \tag{3}$$

Equation 3 is used to determine the Angular acceleration (α) of a body in motion. This acceleration is calculated by dividing the total change in angular velocity (ω) by the change in (t). The angular acceleration will play a key role in the dynamometer because the angular acceleration will reveal how quickly the vehicle may accelerate the dynamometer's rollers to a specific speed.

$$I = \frac{1}{2}mr^2 \tag{4}$$

Equation 4 is used to determine the Mass Moment of Inertia (I) of a body. This inertia is dependent on the mass (m) and the radius (r) of the body or dynamometer's rollers. Note that there are many equations for determining the mass moment of inertia depending on the physical properties of the body, i.e. rectangular, spherical, hollow, and many others. The inertial based dynamometer will focus on the application of solid rollers and thus the corresponding mass moment of inertia equation must be used. The inertia may be defined as the resistance of any physical object to change in its state of motion, which will be applied to the rollers of the dynamometer.

$$\tau_{net} = I\alpha \tag{5}$$

Equation 5 is used to determine the Net Torque (τ) produced by a body in motion. The net torque is calculated by multiplying the mass moment of inertia (I) by the angular acceleration (α). The torque calculated may be defined as the measure of the turning force of an object. This calculated torque will reveal how much torque is being produced at the wheels of the vehicle assuming that the tires of the vehicle and the dynamometer rollers will act as a coupled system.

$$P = \tau * \omega \tag{6}$$

Equation 6 is used to determine the Power Output (P) of the vehicle. The power output is calculated by multiplying the torque (τ) by the angular velocity (ω). The calculated power output will reveal how much power is being produced at the wheels of the vehicle. The power output measurement may expose the presence of unknown factors that may be inhibiting a vehicles maximum performance.

PROCEDURES AND METHODS

Overview

The design of an ideal unit requires a series of components capable of synergizing together to properly obtain accurate results. In order for the system to function consistently from trial to trial, a series of variables must be identified and understood. The series of parameters that would govern the design of the dynamometer include adjustable testing features, safety, as well as clear and concise results. Constructing a simple, light weight, convenient system was of the utmost importance so that the final product may be used and understood by those not of engineering disciplines. Each component of the unit was carefully analyzed and revised from the design stage to the construction stage to ensure an adequate final product. Additional factors such as economics and practicality would also limit the material availability during conceptual design. To evaluate the prototype unit, a series of tests were conducted on four different radio control vehicles of varying classes: Tekno SCT410 (1:10) and the Team Associated RC8.2e RTR (1:8).

Design Procedure

The initial dynamometer design was created using SolidWorks 3D CAD modeling to produce a scale drawing of the conceptualized dynamometer shown below in Figure 3. This particular utilized a basic rectangular frame layout as a base. A series of four knurled rollers would be used under each of the four vehicles tires on a uniform shaft. The shaft would be free to rotate within a series of high speed bearings which are press fit into a system of bearing carriers. The vehicle would then be retained using two straps capable of tensioning through the use of a screw and butterfly nut configuration.

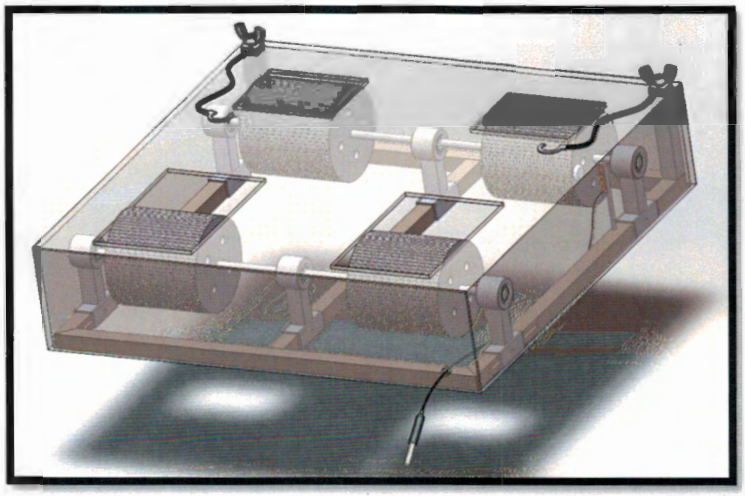

Figure 3. Stage 1 Dynamometer Design

In order to measure the RPM of the rollers on the frame, a magnet will be placed on the side plane of the roller, shown below in Figure 3. A corresponding magnetic coil would also be placed directly across from the rotational path of the magnet on the roller. This magnetic coil would be constructed using a series of copper windings with subsequent layers around a ferromagnetic coil to receive the induced magnetic pulse of the magnet. This will allow for the most powerful signal, while minimizing signal noise. This coil will then feed to an audio jack, visible in Figure 4, capable of being plugged into a computer or laptop to be interpreted by the SimpleDyno software.

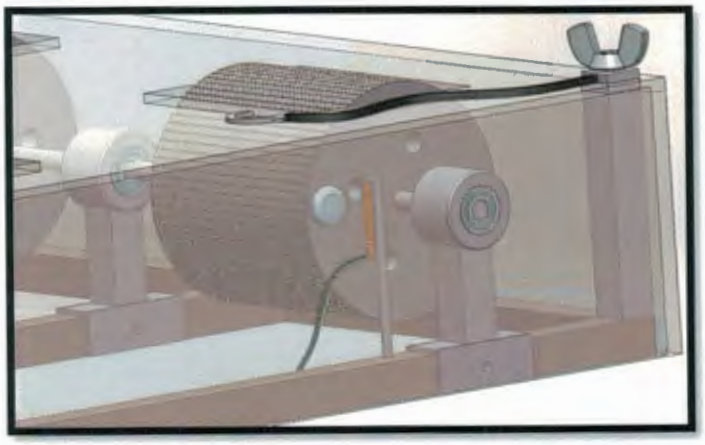

Figure 4. Rear Rollers with Ferromagnetic Coil

The following variable which must be accounted for is the variation of vehicle wheelbases among RC vehicles. Depending on the scale of the vehicle, 1:16 to 1:8, the difference in wheel bases may range anywhere up to 6 inches. Thus, a slot shown in Figure 5 has been placed in the framework to allow for a wheel base range of 9 ½ to 15 ½ inches.

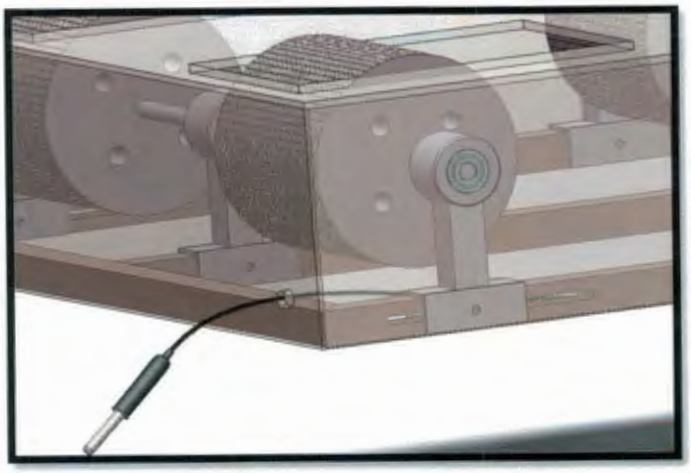

Figure 5. Front Rollers with Slotted Frame

Stage 2 Dynamometer Design

The original design concept was used to develop the first portion of the dynamometer frame and basic components. It was important to assess the material that would be used in construction first hand and consider revising specific design points which will be explained with the visual aid of Figure 6.

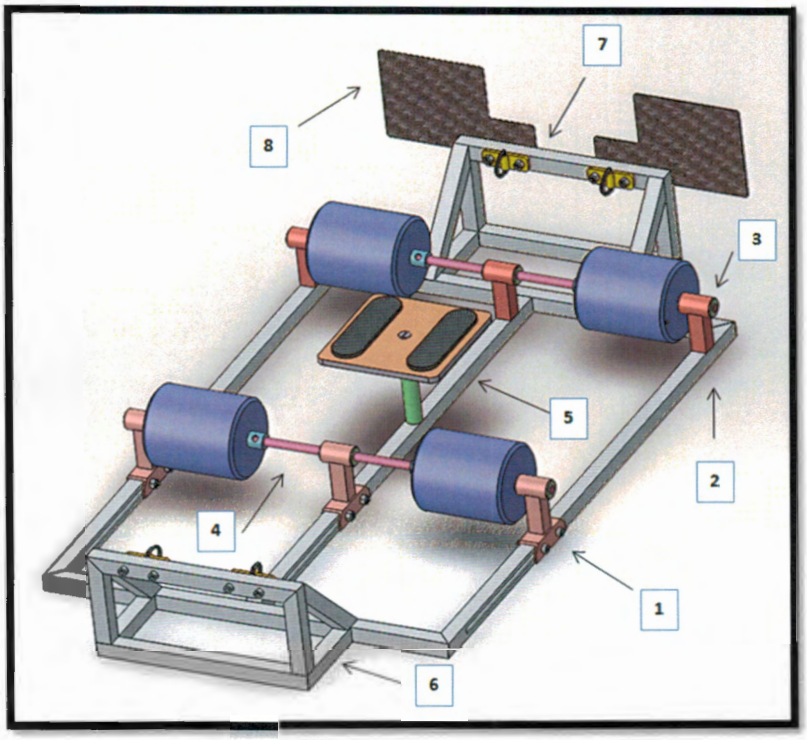

Figure 6. Stage 2 Dynamometer Design with Corresponding Changes

1. The front bearing carrier stands were increased in length to allow two screws to pin the carrier to the frame and in essence increase stabilization through the slotted section.
2. The rear carriers were instead welded directly to the frame instead of bolting to increase durability and reduce potential vibrations.
3. The bearing housing of the carrier assembly was increased in total length from ½" to 1" to prevent deflection of the inner pipe wall due to weld penetration. By preventing this effect, the bearings could be appropriately pressed into housing with the intended interference and minimize any external stress on the bearing once pressed.
4. The roller shaft position will now be retained using a shaft collar and set screw to allow the rollers to be positioned on the inside and the outside of the shaft for varying vehicle widths.
5. A center adjustable turn table will be added to allow for convenient placement of the vehicle onto the dynamometer by a single individual.
6. The front and rear retention system was also revised after the first trial to allow for a stronger design. The pull force of the RC vehicle during acceleration and top speed was much greater than anticipated and thus a truss design was incorporated.

7. A series of bolt on D-clips will mount directly to the top portion of the truss and ¼" ratchet pulleys will be used. These pulleys will attach diagonally to the front and rear of the vehicle to minimize lateral movement of the vehicle during operation.
8. Two rear projectile shields were placed behind the rear rollers to deflect any loose media from escaping from the rubber of the tires and causing potential injury.

The completed revised design may be observed from different viewpoints to allow for reader competency of the applicable revisions. The completed SolidWorks 3D CAD drawing of Version 2.0 may be seen below in Figures 7 and 8.

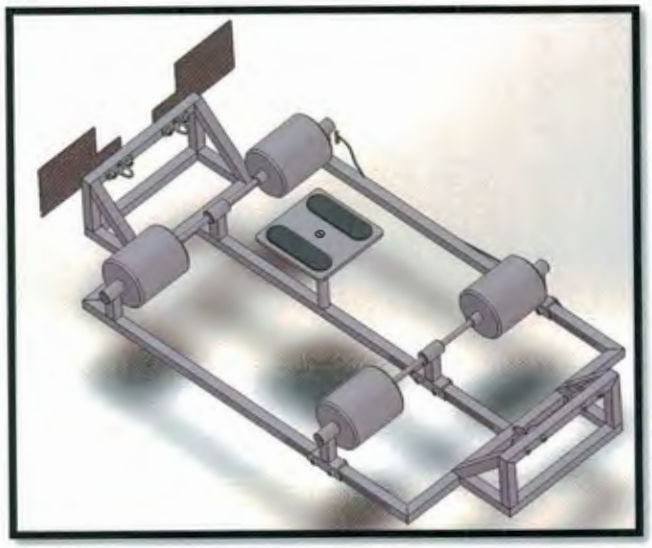

Figure 7. Stage 2 Dynamometer Top View

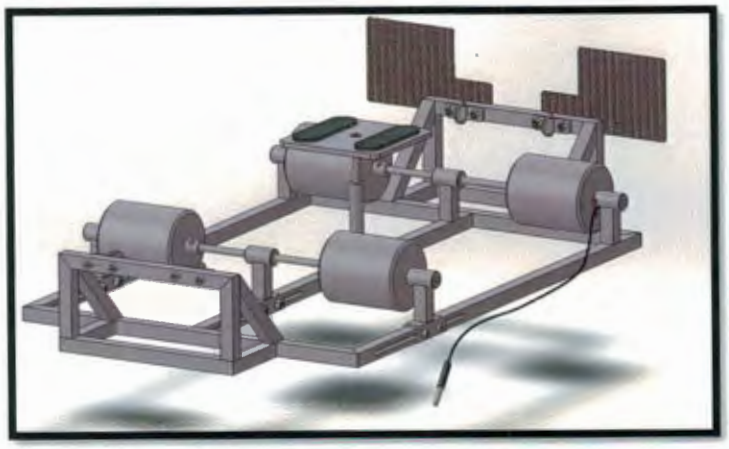

Figure 8. Stage 2 Dynamometer Isotropic View

Software Analysis

The SimpleDyno software is a public program available for download and will be used to quantify and analyze the properties of the vehicle measured on the dynamometer. Through a series of magnets, one on the side of the rear roller and an enamel coated copper wire with corresponding ferromagnetic core, are located on the same rotational path of the roller. The receiving coil magnet is then placed some distance away from the magnet located on the side of the roller and connected to an audio jack. This allows the coil magnet connect directly with the input microphone port on any common computer. With the aid of the software, magnetic pulses are induced upon the magnetic coil and read with the detection channel. Therefore, as the roller increases in rotational speed, the pulses occur more often and the software reads the number of pulses within a given time period and can generate a corresponding RPM. Using this known RPM, the software can then identify the change in the number of pulses within a given time to calculate a corresponding angular acceleration. With the provided mass moment of inertia of the rollers and the measured angular acceleration, the torque produced by the vehicle may then be computed. Due to the nature of the inertial dynamometer, these rollers must be accelerated as quickly as possible to produce the greatest torque output.

In order to size the rollers for both the dynamometer and the SimpleDyno software, a target mass moment of inertia must be developed. A general rule of thumb for rollers used on RC dynamometers is to develop the combined weight of the rollers to be twice the weight of the vehicles to be tested. After weighing a variety of 1:8 and 1:10 vehicles the average weight was determined to be 6 pounds. As a result, a combined weight of 12 lbs was used to govern the dimensions of the rollers.

Using the outputs determined above, four rollers with diameter 2.5 inches and length of 3 inches will create the appropriate roller. This predetermined roller size must then be used to generate a target mass moment of inertia to ensure proper dimensions. Using both Equations 4, 7, and 8 below, as well as the provided mass moment of inertia calculator within the SimpleDyno software in Table 1, the target mass moment of inertia was determined.

$$Volume = \left(\frac{\pi d^2}{4}\right) * l \tag{7}$$

Where,

$\pi = 3.14$

d = Diameter (m)

l = Length (m)

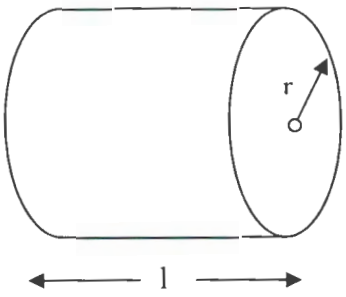

$$Volume = \left(\frac{\pi(.0635\ m)^2}{4}\right) * (.0762\ m) = .00024\ m^3$$

$$Mass = V * \rho \tag{8}$$

Where,

V = Volume (m^3)

ρ = Density of Steel (8050 kg/m^3)

$$Mass = (.0024\ m^3) * \left(8050\ \frac{kg}{m^3}\right) = 1.94\ \frac{kg}{roller}$$

$$I = \frac{1}{2}(m)(r^2) \tag{4}$$

Where,

I = Mass Moment of Inertia ($kg*m^2$)

m = Mass (kg)

r = Radius (m)

$$I = \frac{1}{2}\ (1.94\ kg * 2\ Rollers) * \left(\frac{.0635\ m}{2}\right)^2 = \mathbf{.0019\ kg * m^2}$$

Using the results previously determined, the computed mass moment of inertia is compared against the value determined using SimpleDyno's calculator in Table 1 below.

Table 1. Mass Moment of Inertia Calculator

TARGET MOI			SOLID (ON AXIS)		
Outer Radius Meters	Car Mass Kilograms	Target Roller MOI Kg.M^2	Outer Radius Meters	Roller Mass Kilograms	Solid Roller MOI Kg.M^2
0.0318	2.720	0.0027419	0.0318	3.8800	0.001955641
		0.0000000			0.000000000
		0.0000000			0.000000000
		0.0000000			0.000000000
		0.0000000			0.000000000
		0.0000000			0.000000000
		0.0000000			0.000000000
		0.0000000			0.000000000
		0.0000000			0.000000000
		0.0000000			0.000000000
		0.0000000			0.000000000
		0.0000000			0.000000000
		0.0000000			0.000000000
		0.0000000			0.000000000
		0.0000000			0.000000000
		0.0000000			0.000000000
		0.0000000			0.000000000
		0.0000000			0.000000000
TARGET MOI		0.002	SOLID TOTAL MOI		0.0019
TARGET MOI	(x10000)		0.002		

Therefore the computed value of .002 $kg*m^2$ for the mass moment of inertia was also verified using the provided SimpleDyno software.

Fabrication Procedure

The first process to begin the construction phase is following the appropriate cut list. Each section of the frame is to be cut to create a miter joint in the corners of the frame. This joint may be seen below in Figure 9. A center member is cut with flat ends and is to be placed within the frame to add additional rigidity to the base of the frame.

Figure 9. Frame Miter Joint

In order to ensure that the frame is square after the 45 degree cut, each piece is clamped to a table and measured with a carpenter's square. Once the frame has been assembled, a 1:10 scale vehicle is placed within the frame to test the dimensions as well as the positioning for the adjustment slots which may be seen in Figure 10 below.

Figure 10. Dynamometer Basic Frame Assembly

Following the frame testing, each of the three longitudinal pieces is placed in a mill. Each edge is located and the corresponding 6 inch slot is milled entirely through the aluminum tubing shown in Figure 11.

Figure 11. Milling Frame Slot

Once each of the three longitudinal pieces of tubing has been milled out, the entire frame is fixture together and tig welded. In Figure 12 below, one can see that each of the joints has been welded on both the top and bottom. Due to lack of tig welding experience, each of the inner and outer fillet welds were avoided to prevent any unnecessary damage to the structural pieces.

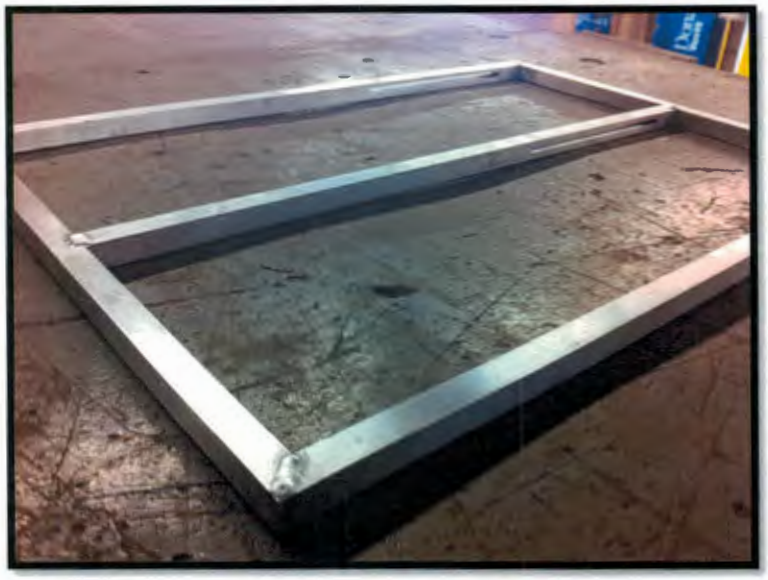

Figure 12. Welded Complete Lower Frame

The rollers were first centered and turned down on a lathe to ensure a perfectly cylindrical surface was present down the entire piece of steel. In Figure 13 below, one may see that the surface of the steel was then knurled to a consistent texture to minimize slip between the tires and the rollers and create accurate results.

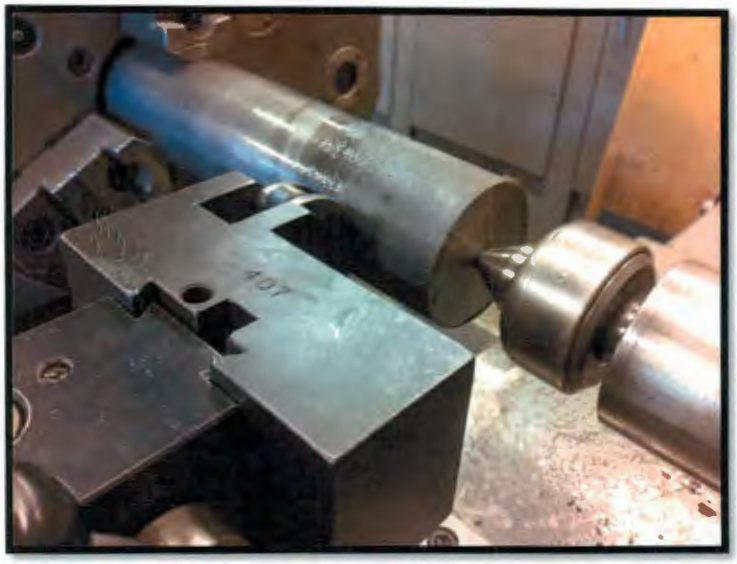

Figure 13. Roller Knurling Process.

Once the entire steel cylinder had a consistently knurled surface, the cylinder was cut into four 3 inch sections. Each of these four cylinders may be seen in Figure 14 below and each of the centers were bored out to receive the main shaft.

Figure 14. Individually Segmented Roller

The assembly of the bearing carriers began by cutting aluminum pipe to the appropriate length. These bearing housings were then pressed into a piece of saddled aluminum tubing and tig welded. In Figure 15 below, one may observe that the weld does not encroach on the section of the pipe that will receive the bearing. This is to prevent internal deformations due to weld penetration and lead to a poor bearing press.

Figure 15. Welded Rear Bearing Carrier Assembly

The following slider guides were fabricated using 1/16" aluminum flat stock and chamfered for cosmetic satisfaction. In Figure 16 below, one may observe that two oversized M4 bolt holes were drilled so that two M4 bolts may attach the bearing carrier through the frame sliders.

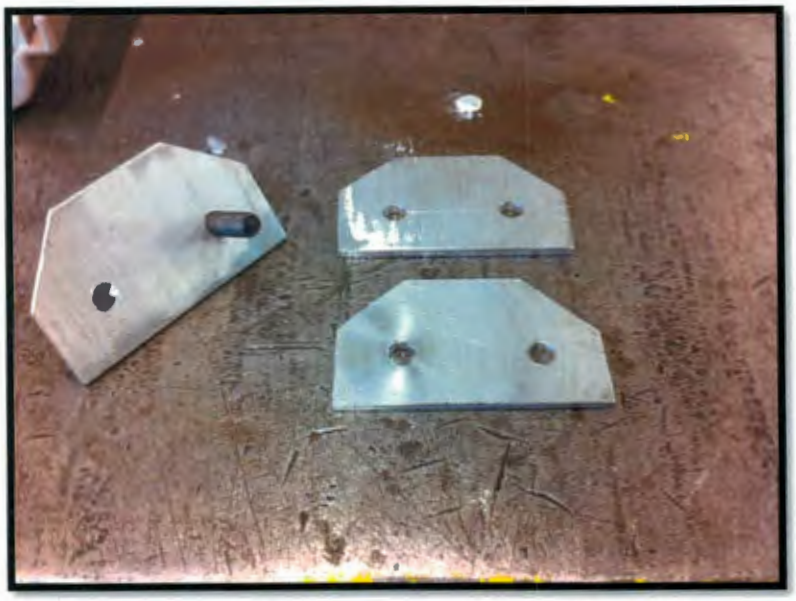

Figure 16. Lower Bearing Carrier Sliders

The bearing carrier assembly was then bolted to the frame and leveled to ensure that the rollers would remain level across the frame. Figure 17 below shows the pre-weld assembly of the bearing carrier on the frame.

Figure 17. Front Sliding Bearing Carrier Assembly

With the three front bearing carriers welded to the corresponding sliders, the bearing press process began. Using a heat gun, the bearing housing was heated to allow the aluminum to undergo a process known as thermal expansion. In the mean time, the bearings were placed in a freezer so that they may experience thermal contraction. The combination of the heated metal and frozen bearings reduces the natural interference between the two components. Using a mini arbor press shown in Figure 18, the bearing was removed from the freezer and pressed into the heated housing. Aluminum was placed underneath the previously pressed bearing to prevent any damage to the bearing as the next bearing was pressed into the opposite side of the housing.

Figure 18. Bearing Heating and Press Process

Once each bearing had been pressed into the appropriate bearing housing, each of the components were placed into their respective positions and adjusted first hand to best fit the vehicles. In Figure 19 below, it is clear as to how the Tekno SCT410 vehicle will stand on the dynamometer.

Figure 19. Dynamometer Layout Test

The bearing carriers were then fixtured to the frame to prevent any change in position as a result of the tig welding process. Shown in Figure 20 below, the roller shaft and rollers are fed through the bearings to ensure that bearings will remain concentric. With the rigidity of the shaft and the weight of the two rollers, the bearing carriers were virtually unable to move. A total of six fillet welds were placed between the two components to ensure structural integrity during loading conditions.

Figure 20. Dynamometer Welding Fixture

With the rear bearing carriers welded to the frame, both the front and rear rollers and corresponding components were assembled. The current frame assembly may be seen below in Figure 21 below with a 1:8 scale RC8.2e buggy for scale.

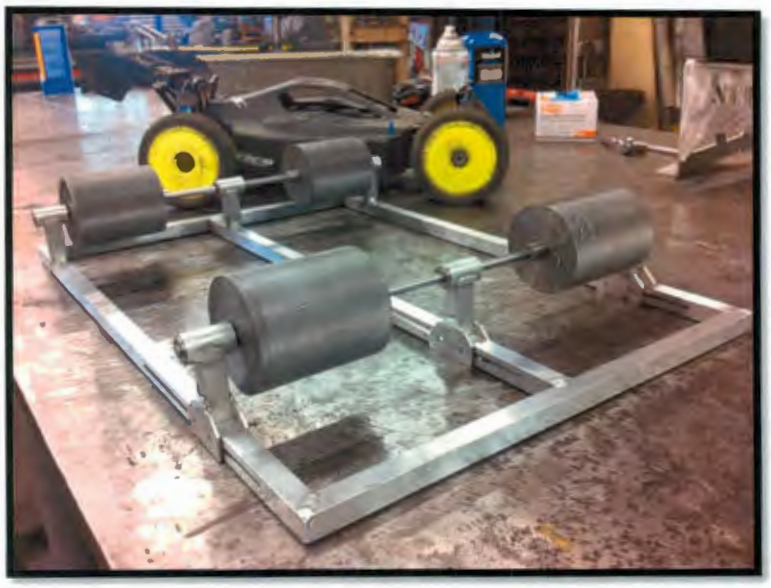

Figure 21. Assembled Basic Dynamometer

A shaft was faced, bored, and welded to the frame to receive a ¼" shaft to telescope vertically and meet the underside of the vehicle's chassis. Shown in Figure 22 below, the side of the receiver shaft was drilled a hole and tapped for an M4 set screw to maintain the position of the inner shaft. The inner shaft was also bored out and tapped to receive an M4 screw and retain the plexiglass table top.

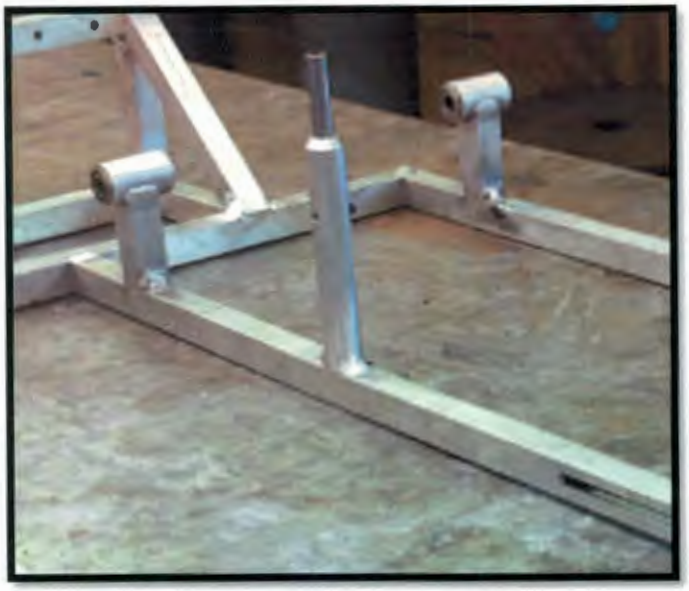

Figure 22. Welded Telescoping Shaft Assembly

Additional aluminum tubing was cut and welded to extend from both the front and rear of the frame. Each of the joints shown in Figure 23 below were welded and then ground down to be flush with the frame surface. This will allow the vertical members of the retention frame to sit flat atop the welded surfaces.

Figure 23. Welded Lower Retention Frame

The upper member of rear retention frame was cut and a series of five holes were drilled into the member. Four of these holes may be seen in Figure 24 below, which will allow for the rear projectile guards to be bolted onto the retention frame. The fifth hole was drilled to receive a ¼" shaft that was bored and tapped for an M4 screw.

Figure 24. Rear Upper Retention Member

This sleeve was then heated and pressed into the member, which may be seen in Figure 25, so that the compression wire clamp system may be used. The underside of this sleeve was also welded to the frame to ensure that sleeve will never spin within the friction press fit while threading in screws.

Figure 25. Heating and Pressing Sleeve

A section of aluminum channel was then cut to an appropriate width and a series of three holes were drilled. The first hole was oversized to allow for an M4 screw and the remaining two holes would allow for the wire to pass through the rear face of the channel visible in Figure 26 below.

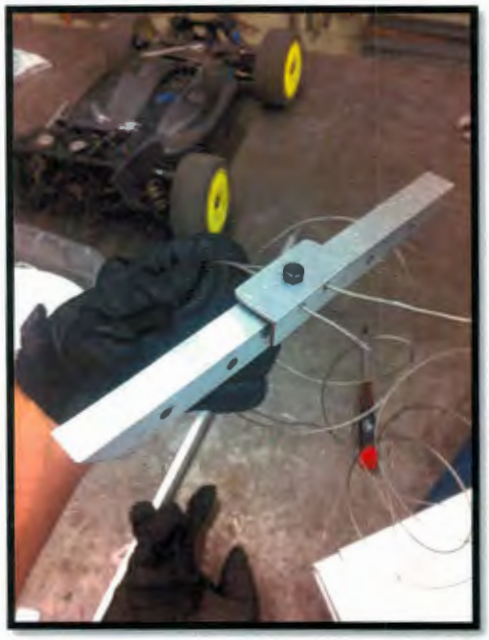

Figure 26. Cable Compression Channel

With each of the sleeves pressed in, each of the miter joints were welded and ground down to allow the rear projectile deflectors to sit flush on the surface. It was very important to ensure that each of the components shown in Figure 27 remained square so that they remain flush with the lower portion of the retention frame.

Figure 27. Upper Retention Frame

In order to weld the vertical portion of the retention frame to the lower portion, each piece was secured through a series of clamps. Additional plates were clamped to the sides of the vertical portion, seen in Figure 28 below, to prevent these members from bowing out past the lower portion of the retention frame.

Figure 28. Retention Frame Welding Fixture

Once the vertical portion of the retention frame was welded to the lower portion, a series of cross members were welded in. Shown in Figure 29 below, each end of the cross member was cut at a 45° angle to maximize the weldable area between each of the members.

Figure 29. Retention Frame Cross Member

Each of the four cross members was welded to both the front and rear retention frame and the completed retention framework may be seen in Figure 30 below.

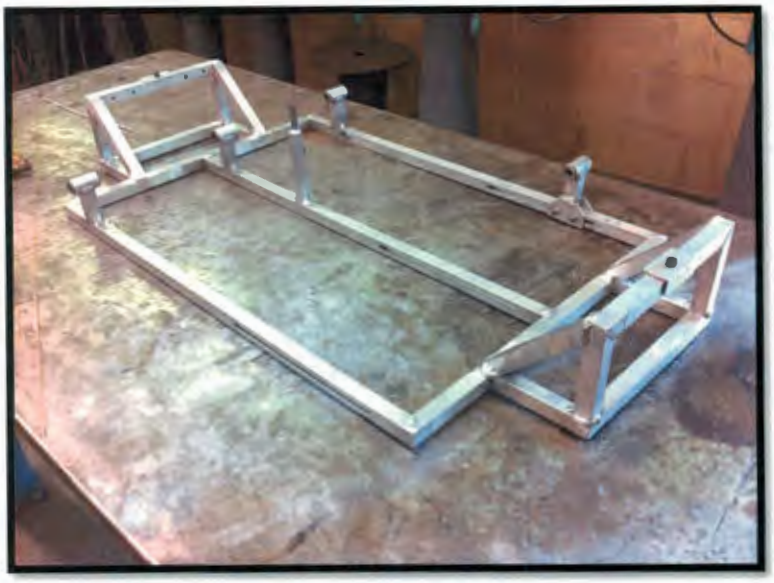

Figure 30. Completed Retention Frame

A ¼"shaft was then bored out and tapped to receive an M4 screw to house the copper coil that will receive the magnetic pulse. Additionally, a ¼" hole was drilled into the frame so that shaft may be press fit into the frame. While drill holes do not provide optimum tolerances for press fitting, the coil mount is not structural and will suffice in these given conditions. The positioning of the hole was determined by placing the magnet on the side of the roller, seen in Figure 31, and observing the path of the magnet as the roller spun.

Figure 31. Sensor Mounting Shaft

In order to properly secure the magnet to the side of the roller, a hole was drilled into the side of the roller. Using an epoxy compound seen in Figure 32, the hole was then partially filled with epoxy and the magnet was pressed into the roller. This would ensure that magnet is incapable of falling from the press fit.

Figure 32. Magnet Epoxy and Press

Two pieces of 100 pound rated steel braided wire were used to construct the front and rear retention cables. A total of three cable clamps were used for each wire and were compressed using a wire clamp seen in Figure 33 below. A clamp was placed at the end of each hook as well as the end of the wire to create a convenient pull loop for tensioning.

Figure 33. Wire Clamp

A single carbon fiber sheet was used to create the rear projectile deflectors that are to be placed behind the vehicle. In Figure 34 below, a 20° angled cut was made on the inside corner of the deflectors to allow clearance for the rear spoiler mounts on any buggy class vehicle. Two corresponding holes were also drilled into the deflectors to allow the deflectors to be mounted to the retention frame.

Figure 34. Carbon Fiber Projectile Deflectors

With the fabrication of the dynamometer complete, the surface of the frame was sanded to remove minor scratches and imperfections. Using both a 150 and 300 grit sand paper the surface of the frame was wet sanded and finished with a scotch bright pad. The finished surface of the frame may be seen in Figure 35 below.

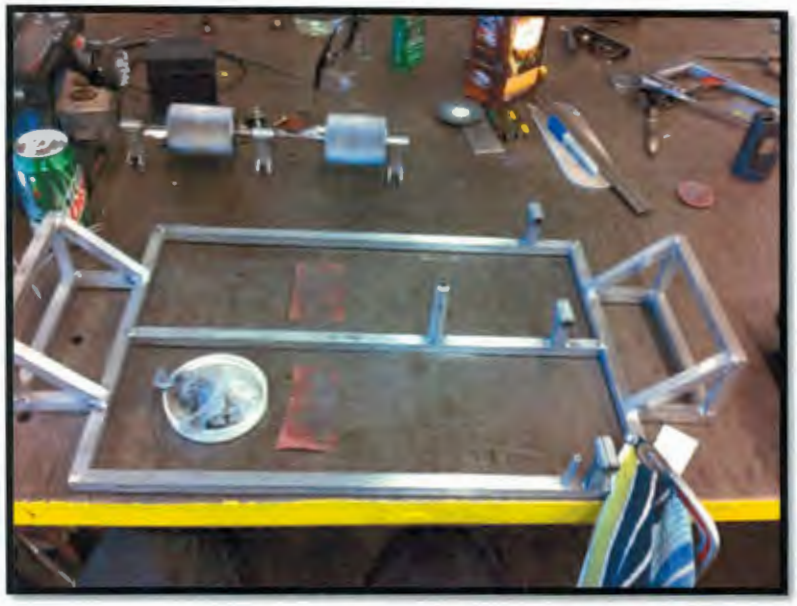

Figure 35. Dynamometer Frame Sanding

After the surface of the frame was sanded and finished, aluminum polishing cream was applied to remove the oxidation. The cream was applied using terrycloth and gently applied until the surface reached a mirror finish evident in Figure 36.

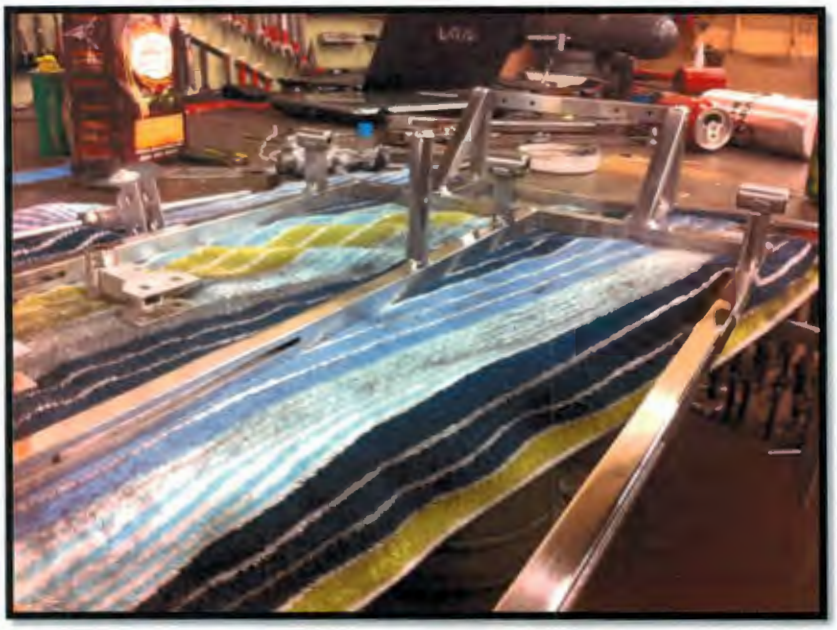

Figure 36. Dynamometer Frame Polishing

Once the entire dynamometer was polished and cleaned of any residue present, each component was reassembled. The completed dynamometer may be seen in Figure 37 below.

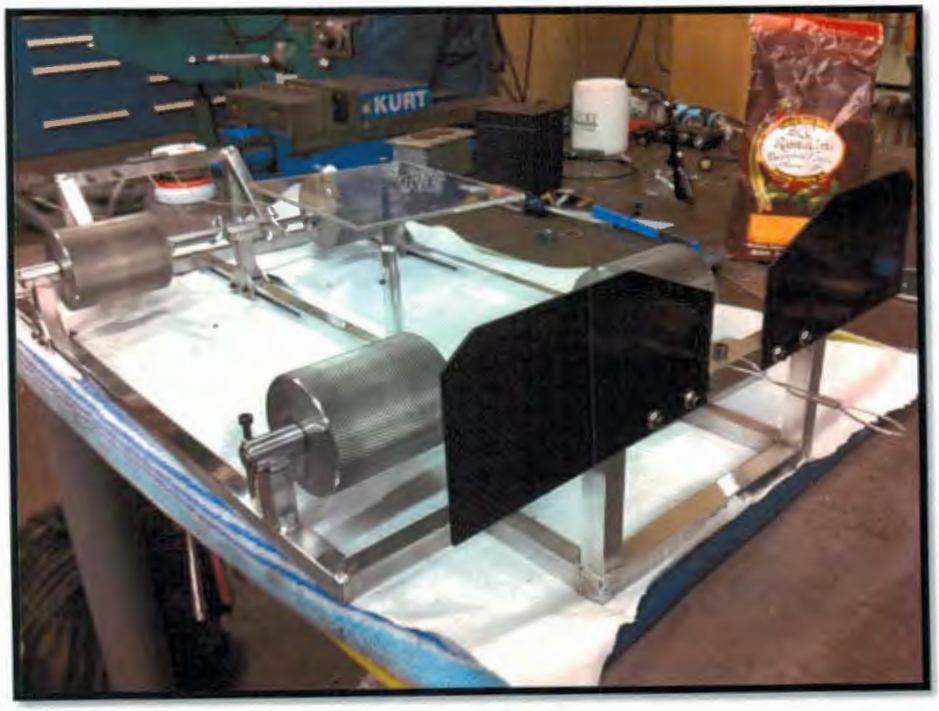

Figure 37. Completed Dynamometer

Testing Procedure

After completing the basic design, it was necessary to test the functionality of the dynamometer prior to continuing with the fabrication process. This stage of testing would reveal how well the bearings could rotate at the induced tire speed and the overall alignment of the roller shaft. If the shaft were not well aligned to the inner diameter of the bearings, an eccentric load would cause an unknown amplitude stress. This process would also reveal how the vehicle itself will behave on the dynamometer from start to finish.

With the assistance of Dr. Mark Zohns and Mr. Virgil Threlkel, a makeshift restraint system was developed and may be seen in Figure 38. Using a 100 pound rated steel wire and 3/8" bungee cord were hooked to the rear control arms and front shock tower of the RC 8.2E Buggy and down to the work table. Due to the severe angle of restraints, a compressive force was induced on the suspension of the vehicle, inevitably increasing traction and potentially impacting the final results during testing. As the vehicle was slowly throttled up to maximum speed, the minor imbalances within the vehicles tuning caused the vehicle to move laterally across the dynamometer. This motion was too drastic to allow the vehicle to operate independently from assistances and lead to the derivation of the second design concept.

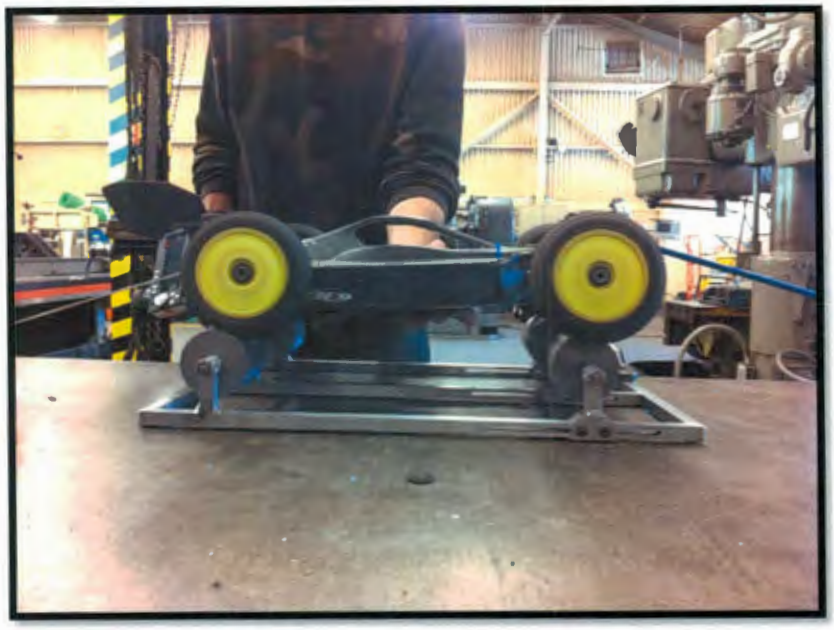

Figure 38. Dynamometer Functionality Test

As a result of the significant pull force observed during operation, a load test was conducted to quantify how much force the RC vehicle was capable of pulling. A spring scale was then used to observe how much pull force could be generated with the SCT 410 vehicle, which is a scale lower than the RC 8.2e buggy. With the assistance of Mr.

Threlkel shown in Figure 39 below, the test was conducted multiple times. On smooth concrete the 1:10 scale vehicle was capable of generating 10 lbs; on the rubber floor mat, the vehicle could produce 11 pounds; and lastly while on carpet, the vehicle was capable of generating 12 pounds.

Figure 39. Load Cell Testing

Concerns arose in regards to the physical construction of the original retention system within the Stage 1 Design, as the stress at the welds may overcome the strength at the lower retention frame. With Figure 40 below, one may observe the basic free body diagram of the loading conditions experienced by the frame.

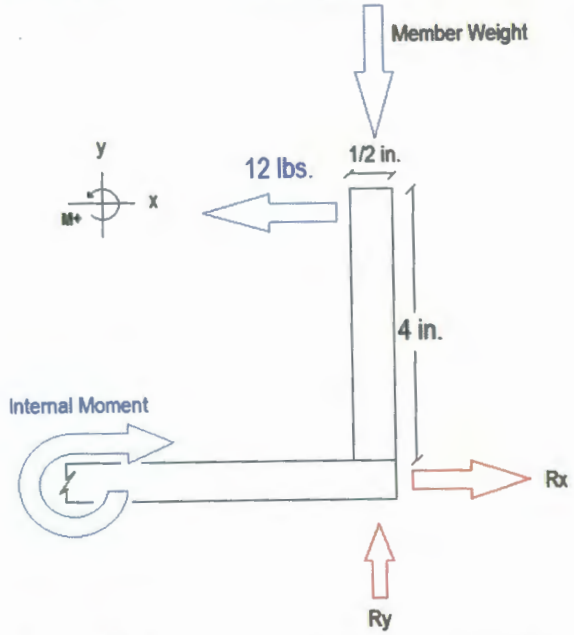

Figure 40. Retention Frame Free Body Diagram

Using Equation 7 below, one may theoretically observe the basic strength of the materials the anticipated loading.

$$\sigma = \frac{MC}{I} \tag{7}$$

Where,

σ = Stress (lb/in^2 or PSI)
M = Moment (in-lbs)
C = Distance to the Neutral Axis
I = Moment of Inertia

$$M = (12\ lb) * (4\ in) = 48\ in * lb$$

$$C = \frac{(\frac{1}{2}\ in)}{2} = \frac{1}{4}\ in$$

$$I = \frac{(\frac{1}{2}\ in) * (\frac{1}{2}\ in)^3}{12} - \frac{(\frac{3}{8}\ in) * (\frac{3}{8}\ in)^3}{12} = .0036\ in^4$$

$$\sigma = \frac{(48\ in*lb) * (\frac{1}{4}\ in)}{(.0036\ in^4)} = \mathbf{3{,}300\ PSI}$$

After determining the anticipated stress that will be present at the weld (3,300 PSI) the design stress must be compared against the ultimate tensile strength. Using Table 1 below, 6061 aluminum has an ultimate tensile strength property of 35 to 45 ksi. However, due to welding process, 6061 aluminum loses some of the heat treated properties, thus will behave more similar to 5052, which has a tensile strength property of 20-33 ksi.

Table 2. Aluminum Alloy Properties

Alloy	Nominal Density (lbs./cu. in.)	Modulus of Elasticity, ksi x 10^3	Ultimate Tensile Strength, ksi	Elongation %	Melting Range, °F	Thermal Conductivity @ 77°F, unless otherwise stated (Btu/hr x in./sq. ft.)	Electrical Resistivity @ 68°F (Ohm-Cir. Mil/ft.)
1100, 1145, 1235	0.098	10.0	11-29.7	3-35	1190° to 1220°	1500-1600	16.8-18
2011	0.102	10.2	55-57	10-15	1005° to 1190°	1050-1060 @ 75° to 77°F	27
2017	0.101	10.5	62	22	955° to 1185°	930	31
2024	0.101	10.6	62-70	10-20	935° to 1180°	840 @ 75° to 77°F	30-35
3003, 3105	0.098	10.0	20-29	2-5	900° to 1210°	1100-1500	21-25
4032	0.097	11.4	55	8	990° to 1060°	960 @ 75°F	30
5005, 5205	0.098	10.0	20-26	4	1170° to 1210°	1390	20
5052	0.097	10.0	20-33	4-12	1125° to 1210°	960-1390	20-30
5083	0.096	10.3	44	12	1095° to 1180°	810	10.2
5086	0.096	10.3	40-47	10-12	1085° to 1185°	870	10.2-33
6013	0.098	10.1	55-65	5-11	1025° to 1205°	1140	Not rated
6020	0.098	Not rated	42-52	9-12	1080° to 1205°	Not rated	Not rated
6060	0.098	10.1	27.6-45	10-13	1030° to 1211°	1160-1449	19.25
6061	0.097-0.1	10.0	35-45	8-17	1080° to 1205°	1390 @ 75° to 77°F	24
6063	0.097	10.0	22-30	8-14	1110° to 1210°	1390-1452	15.8-28
6101	0.098	10.0	32	15	1080° to 1205°	96	24
7050	0.102	10.4	76	11	910° to 1165°	1090	25
7068	0.103	Not rated	103	9	Not rated	Not rated	Not rated
7075	0.101	10.4	71-83	9-13	890° to 1175°	900 @ 75° to 77°F	31
MIC6	0.101	10.3x10^6	24	3	1200°	984	Not rated
Porous Mold-Quality	0.065	1.3	Not rated	Not rated	Not rated	Not rated	Not rated
QC-10	0.103	10.4	82	10	1050°	1104	Not rated

After reviewing each of the predetermined loads, an analysis of the Factor of Safety must be conducted. Using Equation 8 below, one may observe the limits of the design.

$$Factor\ of\ Safety = \frac{Material\ Strength}{Design\ Load} \quad (8)$$

Where,

Material Strength = 20-30 ksi

Design Load = 3.3 ksi

$$F.S. = \frac{20\ ksi}{3.3\ ksi} = \mathbf{6.0}$$

Concerns also arose regarding torsional deflection within the rear frame member and were then analyzed in Figure 41 and Equation 9 below.

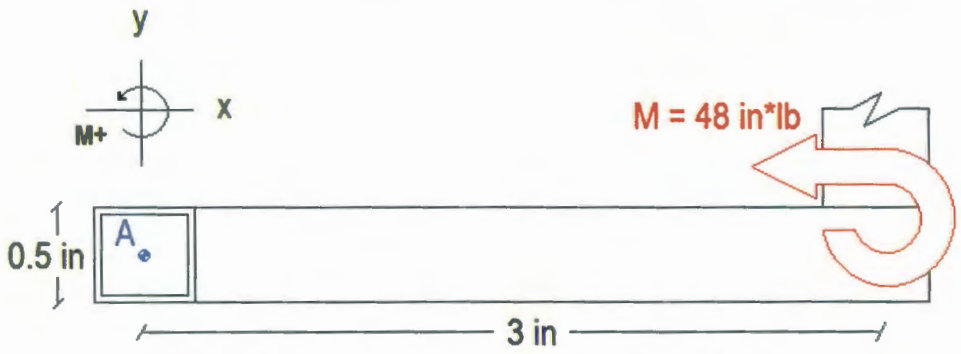

Figure 41. Lower Retention Frame Free Body Diagram

$$\theta_{MAX} = \theta(L) = \frac{ML}{EI} \quad (9)$$

Where,

θ_{MAX} = Maximum Angular Deflection

L = Length (inches)

E = Young's Modulus = 102,000 ksi (5052 Aluminum)

I = Moment of Inertia

$$\theta_{MAX} = \frac{(48\ in * lb)(4\ in)}{(102{,}000\ ksi)(0.0036 in^4)} = \mathbf{0.225\ degrees}$$

A Factor of Safety of 6.0 has and a total rotation deflection of 0.225 degrees has revealed that the design as well as basic material property is more that capable of handling the anticipated loading conditions. Thus the cross members are highly unnecessary to reinforce the restraint system; however, due to tig welding inexperience concerns arose that the welds would not reach sufficient penetration. Therefore, the welds could potentially fail after an extended period of testing trials, thus the diagonal reinforcement members were added.

With the retention system fabricated, it was important to apply the restraint system to a variety of vehicles. By doing so, this revealed that the retention hook diameter is large enough to attach to different points on the vehicle. It was also observed that sufficient offset could be created to develop a cross strap system with the given wire length to prevent the vehicle from moving laterally. Lastly, tension was induced via the wire pull tab and the wires were compressed successfully with the aluminum channel to prevent and slack from returning to the cables which may be seen in Figure 42 below.

Figure 42. Cable Tension Testing

The second testing attempt would reveal how well the vehicle was truly retained atop the central table top as well as whether or not the retention frame could support the pull force generated. As a result, the vehicle was entirely stationary and there appeared to be no visible deflection within the framework. As the vehicle reached full throttle while on the dynamometer, the rear suspension began to significantly compressed, visible in Figure 43 below. As a result, it was clear that the plexiglass table top was bending under the chassis of the vehicle. This, however, was not of major concern, due to the fact that plexiglass is a plastic material and thus contains elastic properties. Additionally, this effect allowed the vehicle to behave much more natural while still being supported by the table top.

Figure 43. Operations Testing

With the basic testing complete, the next step was to incorporate the data acquisition system. The initial parameters were input into the software program and the first basic test was conducted. Due to the incompletion of the sensor mount during testing, a temporary stand was used and the vehicles were not fully engaged on the dynamometer. In Figure 44 below, one may observe the basics of the SimpleDyno interface during one of the software tests.

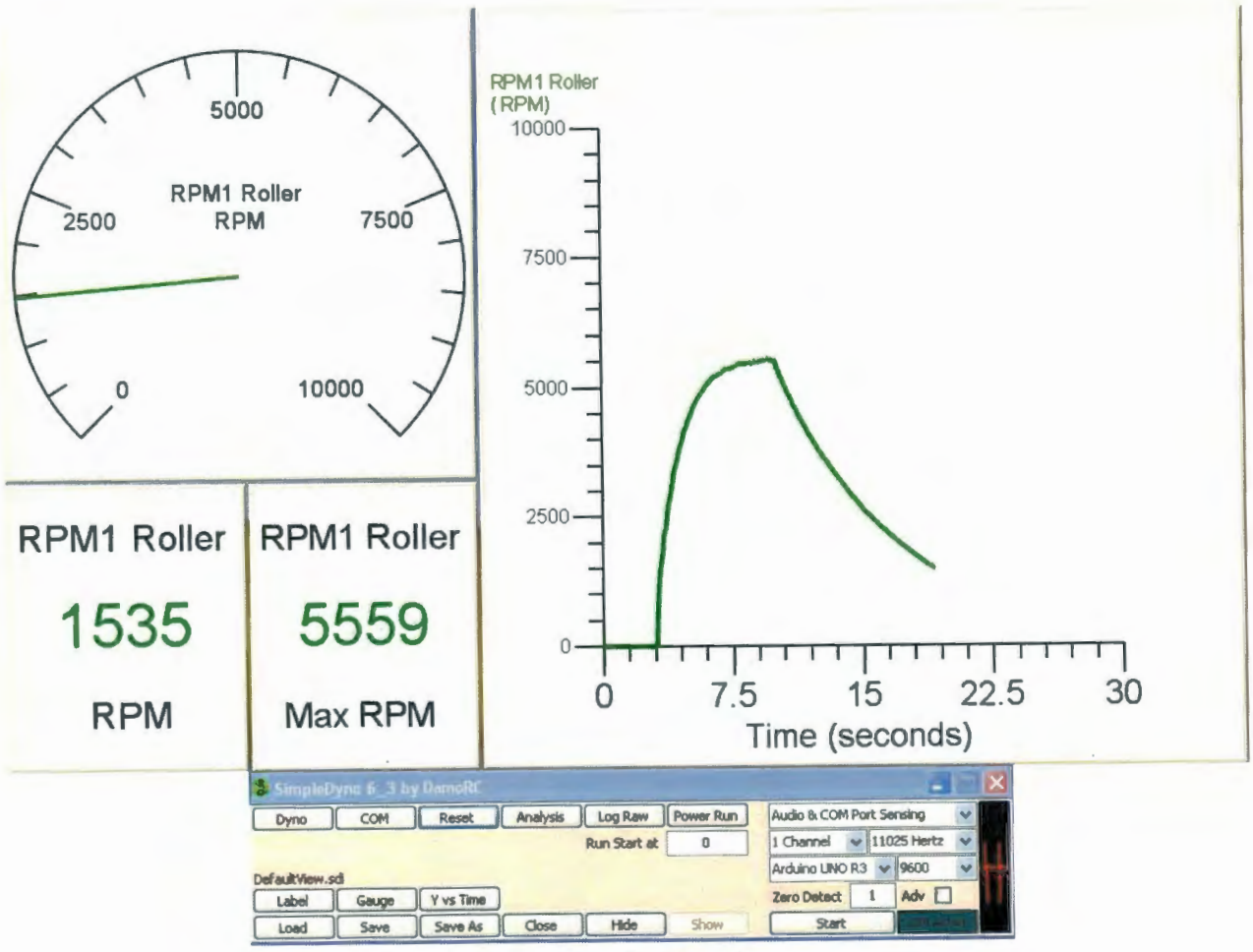

Figure 44. SimpleDyno Test Interface

RESULTS

A series of two tests of both the Team Associated RC8.2e Buggy (1:8) and the Tekno SCT 410 (1:10) vehicles were both tested on the dynamometer and analyzed using the SimpleDyno software. The RC8.2e Buggy utilizes a wheelbase of 12.72 inches and the Tekno SCT410 utilizes a wheelbase of 13.18 inches, thus requiring slight roller adjustment between testing. The performance results can be seen in Figures 45 and 46 below. Within these figures, one may observe the maximum speed each of the vehicles reached during testing, as well as the torque and horsepower. A drag coefficient was also set within the program to model the true performance of each vehicle during use.

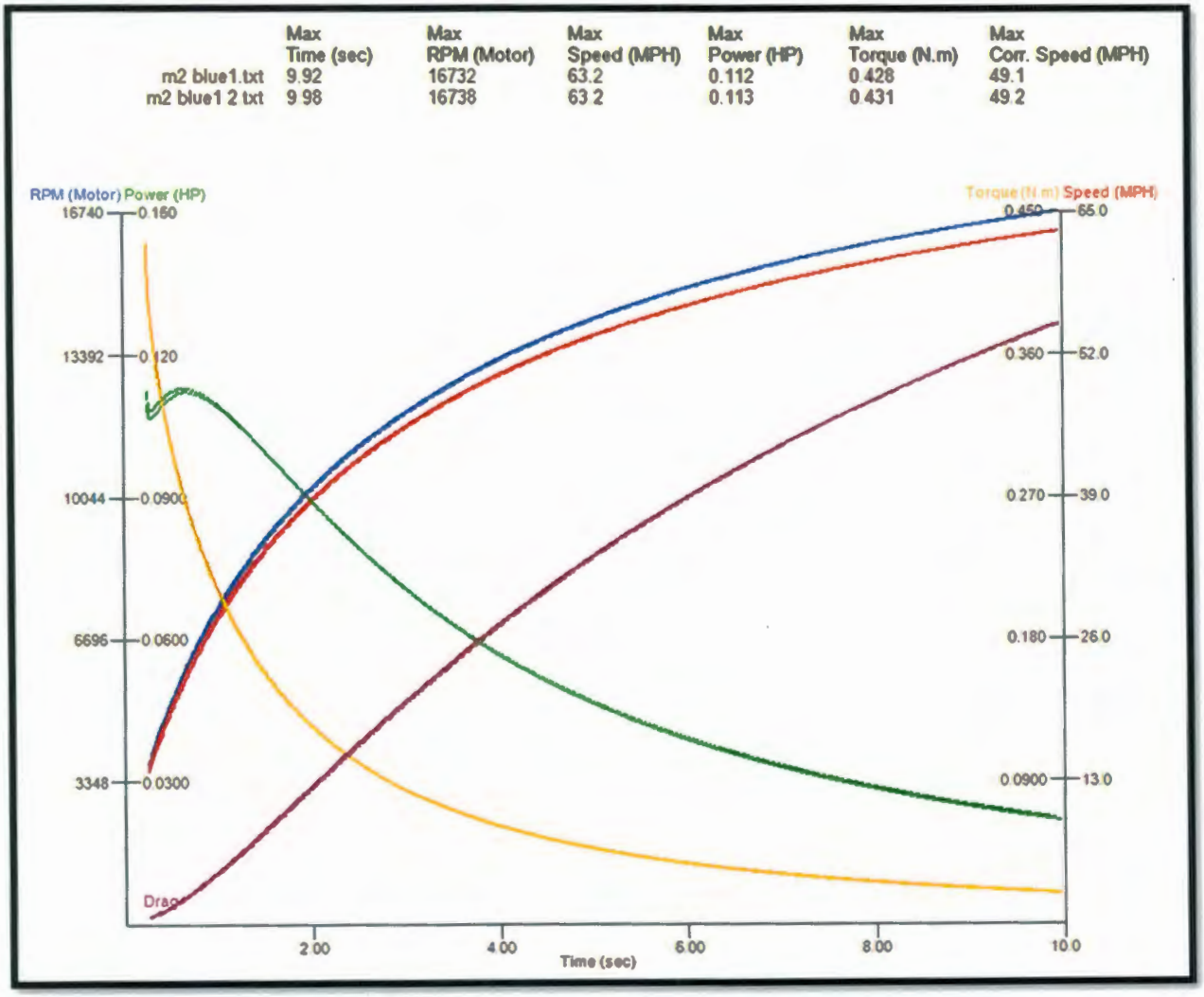

Figure 45. Performance Results of the RC8.2e Buggy

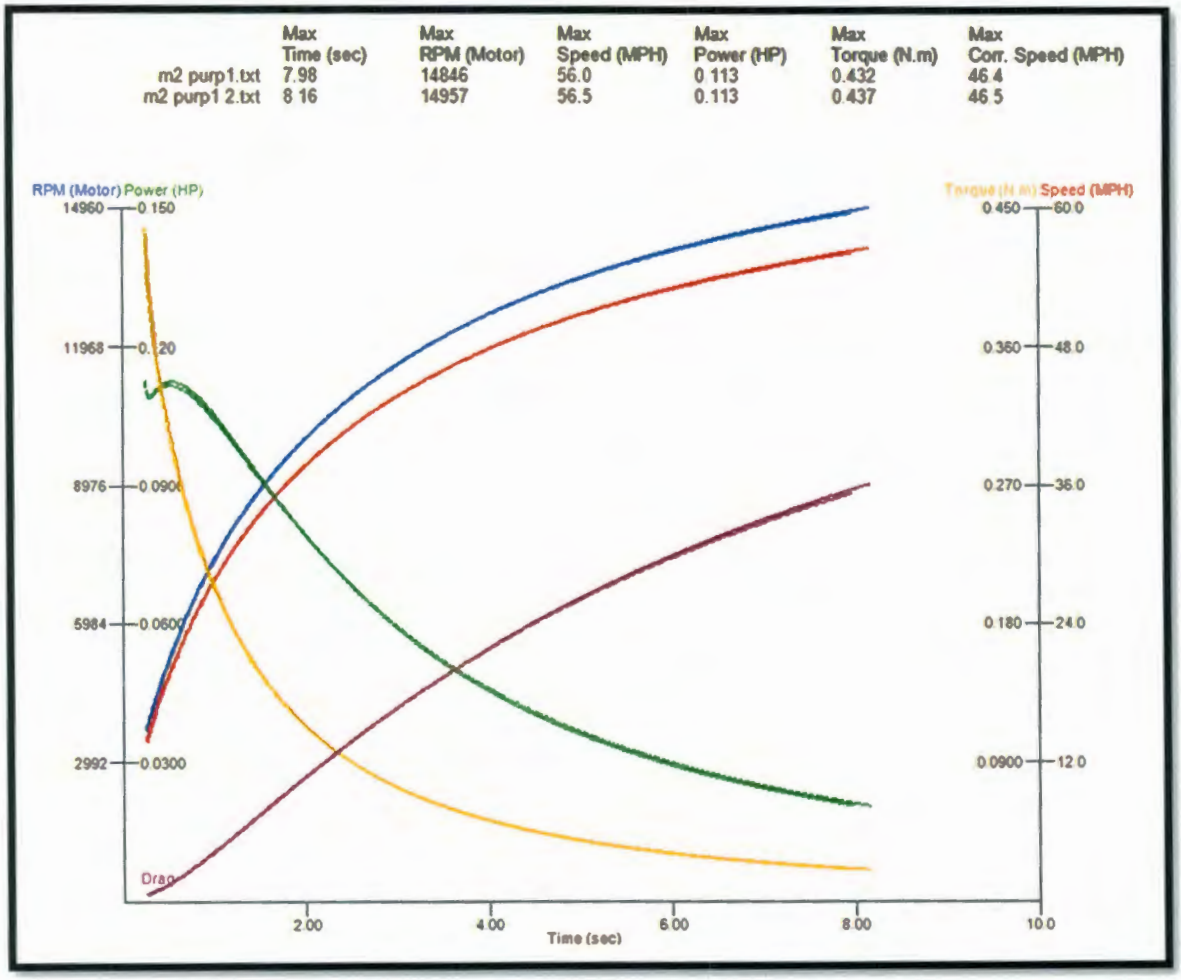

Figure 46. Performance Results of the Tekno SCT410

DISCUSSION

Overview

The data acquisition process of the dynamometer was very simple to use and allowed for a "plug and play" operation evident in Figure 47. The receiving ferromagnetic copper coil output to a standard stereo jack that could be plugged into the microphone port of any laptop or computer. From there, the SimpleDyno software requires a series of parameters to be set regarding the roller dimensions and noncritical parameters regarding the vehicle. Once all of these requirements have been specified, the operator may set an infinite number of combinations of gauges and graphs that display performance characteristics measured on the dynamometer such as current, minimum or maximum torque, speed, and horsepower, as well as many others. Lastly, power analyses may be conducted to present the entire data set on a single graph to see how each performance characteristic changes over the duration of the test.

Figure 47. Dynamometer Testing and Data Acquisition

After reviewing and operating the dynamometer, the device was sufficient in obtaining and quantifying the properties of various RC vehicles. The Stage 2 design required little to no additional changes to finalize the device and conclude the fabrication process. By using ½"x ½"x1/16" aluminum tubing, carbon fiber, and plexiglass, the final device with the steel rollers remained under 15 lbs, making it easy to transport. The cable restraint system keeps the vehicle entirely stationary, making the device very safe and allowing the operator to give full attention to the results being quantified through SimpleDyno. The completed dynamometer may be seen in Figures 48 and 49 below.

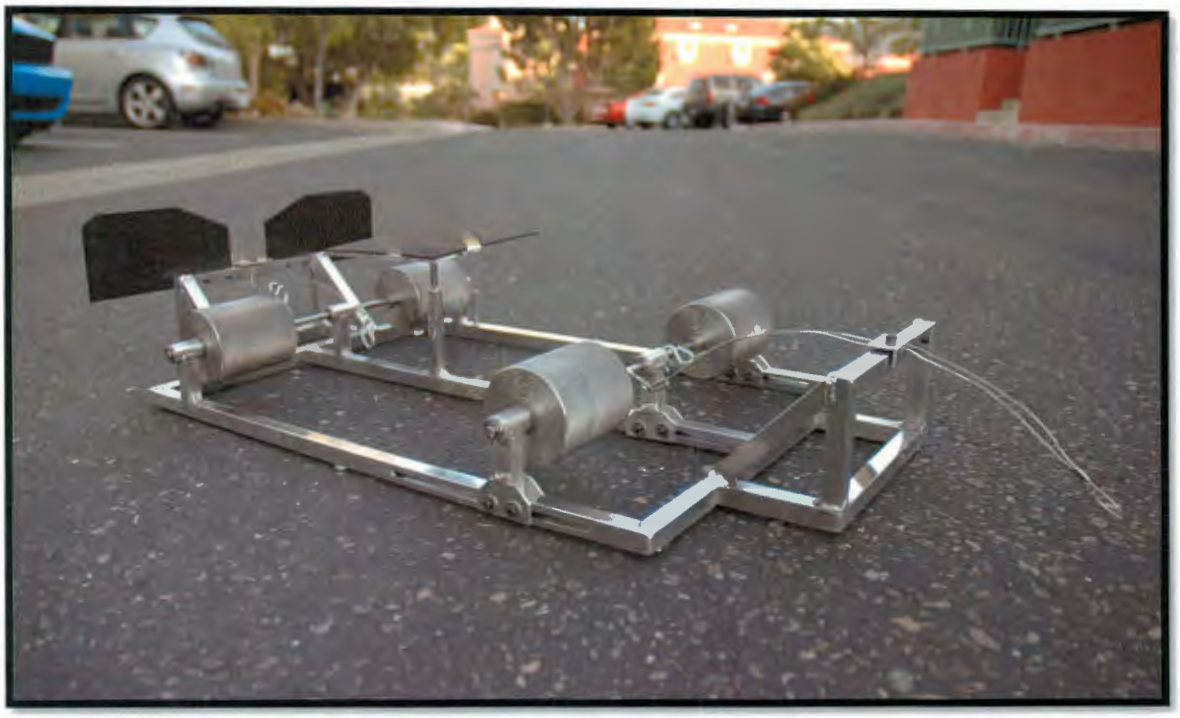

Figure 48. Completed Dynamometer

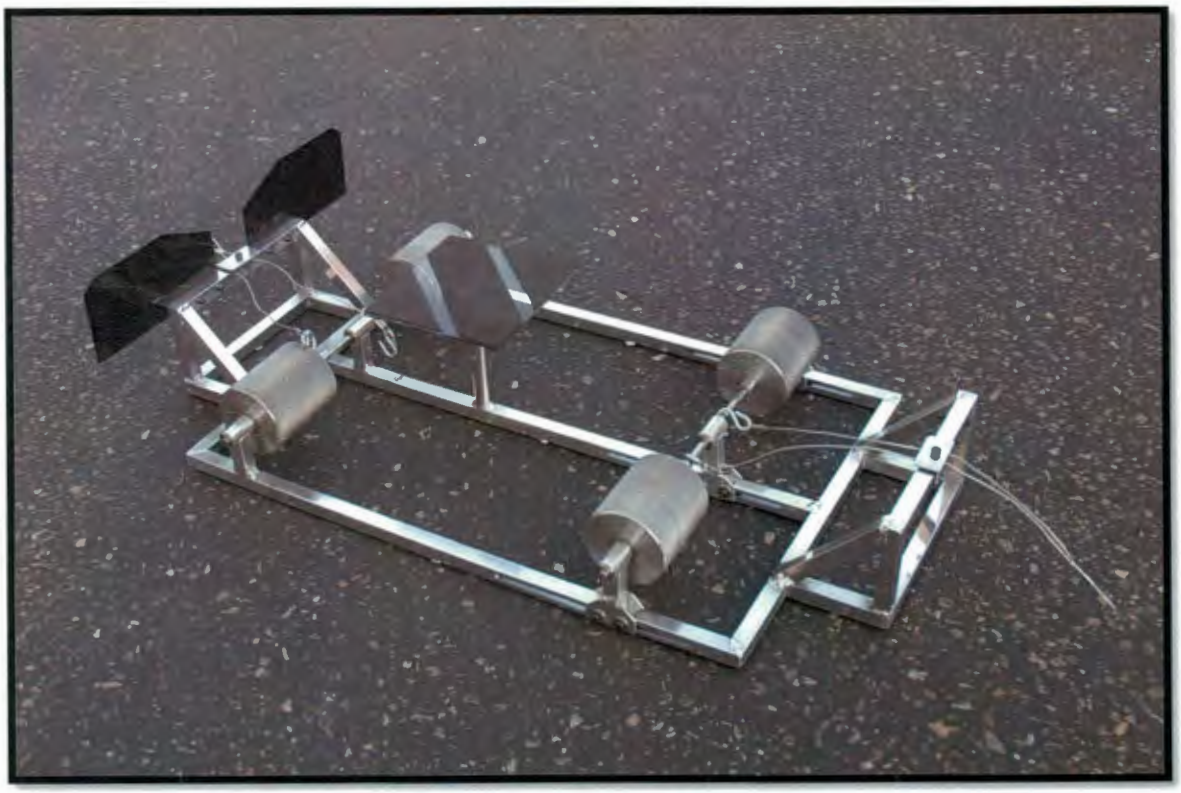

Figure 49. Completed Dynamometer (2)

Cost Overview

After reviewing each component used in the dynamometer for fabrication, the cost of each unit used within the project, as well as the total cost for the raw material was compiled within Table 3. Note that the SimpleDyno software, is a free data acquisition system used to quantify the results obtained from the dynamometer.

Table 3. Materials and Cost List

Part	Quantity	Cost per Unit	Total Cost	Supplier
Avid 1/4" Bearings	12	$ 1.00	$ 12.00	Avid RC
2.5" Dia x 12" Steel Roller	1	$ 49.94	$ 49.94	McMaster Carr
.25" Dia x 36" Roller Rod	1	$ 2.46	$ 2.46	McMaster Carr
.5"x.5" Sq. Al Tubing (6 ft)	1	$ 12.93	$ 12.93	McMaster Carr
.5"x.5" Sq. Al Tubing (3 ft)	3	$ 7.50	$ 22.50	McMaster Carr
.495" ID 5/8" OD Al Round (1 ft)	1	$ 4.03	$ 8.05	McMaster Carr
0.4844" OD Filler Rod (1 ft)	1	$ 3.20	$ 9.60	McMaster Carr
.5" Aluminum Rod (1/2 ft)	1	$ 1.45	$ 2.17	McMaster Carr
.5"x.75" Aluminum Channel (3 ft)	1	$ 0.42	$ 4.99	Ace Hardware
.25" Aluminum Rod (3 ft)	1	$ 0.26	$ 4.59	Home Depot
1/2" Rubber Pads	16	$ 0.19	$ 2.97	Home Depot
Magnet	6	$ 0.66	$ 3.98	Home Depot
Copper Wire	1	$ 3.24	$ 3.24	Home Depot
M4 Set Screw	5	$ 0.29	$ 1.45	Hobby Head Quarters
M4x16mm Machine Head Screw	1	$ 0.55	$ 0.55	Ace Hardware
M4x12mm Machine Head Screw	2	$ 0.31	$ 0.62	Ace Hardware
M4x8mm Tapered Screw	1	$ 0.28	$ 0.28	Ace Hardware
M4 Washer	16	$ 0.21	$ 3.36	Ace Hardware
M3x20 mm Machine Head Screw	6	$ 0.62	$ 3.72	Ace Hardware
M3x25mm Machine Head Screw	6	$ 0.65	$ 3.90	Ace Hardware
M3 Locknut	12	$ 0.23	$ 2.76	Ace Hardware
Carbon Fiber Shield	1	$ 15.81	$ 15.81	McMaster Carr
Plexiglass Stabilization Plate	1	$ 4.29	$ 4.29	Ace Hardware
Foam Platform Top	1	$ 0.99	$ 0.99	Ace Hardware
9' Steel Wire (100 lb rated)	1	$ 1.75	$ 3.49	Home Depot
Steel S-Hooks	4	$ 0.37	$ 1.47	Home Depot
Wire Clamps	6	$ 0.67	$ 3.99	Home Depot
150 Grit Sand Paper	1	$ 1.57	$ 1.57	Ace Hardware
300 Grit Sand Paper	1	$ 1.57	$ 1.57	Ace Hardware
Scotchbright Finish Pad	1	$ 3.59	$ 3.59	Ace Hardware
Aluminum Polishing Cream	1	$ 7.99	$ 7.99	Ace Hardware

Total Cost =	**$ 200.82**

As a result, the total cost of raw materials the required to fabricate the dynamometer came to a total cost of $200.82. This cost is located within the lower portion of the $200 to $300 price range originally proposed, allowing it to be an easily available for theoretical market sales. Note that the SimpleDyno software is available online at no cost, thus available to anyone with a computer.

Final Design Modifications

Following the Stage 2 Design concept, various modifications were still necessary to maximize the functionality of the device. The three most prominent modifications and additions to the project consisted of restraint revisions, table top ergonomics, and frame dampening.

The Stage 2 design concept utilized a series of bolt on D-clips paired with a series of ratchet tie down locks. After reviewing the ratchet tie-downs, the devices were deemed too large to be placed on the dynamometer as well as the vehicle itself. As a result, the D-clips were replaced by a threaded sleeve and compression plate. The ratchet tie-downs were replaced by 100 lb rated steel wire and simple stainless steel S-hooks. This revised design allowed for the desired adjustable tension system and still maintained adequacy. In addition, the revised system was more compact, simple, and light weight, reducing inconvenience during use and transport of the dynamometer.

After the second testing of the restraint system, concerns arose regarding the dynamometer remaining stationary during operation. Due to the torque output of the high performance RC vehicle and resulting vibrations, the entire dynamometer would move forward. During one trial of around 5 to 10 seconds in operation, the dynamometer was capable of displacing itself nearly a foot forwards from its initial starting point. This was due to the very low coefficient of friction, μ,that exists between the aluminum dynamometer frame and the steel work bench. In order to counteract this movement, self adhesive rubber pads were placed underneath the dynamometer frame. The presence of these rubber pads prevented the frame displacement that occurred during operation, as well as dampened the vibrations that were ultimately produced.

The final addition to the dynamometer was a 1/16" piece of foam padding to the surface of the central table top. Allowing the underside of the RC chassis make direct contact with the plexiglass surface allowed for too much slip while placing the vehicle onto the dynamometer. The presence of a foam surface allowed the vehicle to remain entirely stationary and prevents dirt and dust from scratching the underside of the RC chassis as well as the plexiglass table top.

Difficulties Encountered

The most prominent difficulty encountered during the fabrication of the project was the use of a tig welder. Since aluminum was selected to compose the frame and the bearing carriers due to its lightweight properties and convenience for press fitting, tig welding was the only available option. The aluminum tubing that was selected (½" x ½" x 1/16") also compounded the difficulty of creating adequate welds through the tig welding process. Aluminum tubing of this size and thickness rapidly conducted the heat created through the welding process and would cause unexpected undercut and eventually material blow out. Ultimately, with enough practice and patience a proper welding technique was developed and the fabrication of the dynamometer progressed.

The following difficulty that arose during the fabrication process was the placement of the 6" slot for the front wheel base adjustment. The slot was cut using a mill and in order to located the center of the aluminum tubing using an edge finder. Due to mill operating inexperience, the edge finder located a center of the tubing that was not the true center. This lead to a slot that was roughly 15 thousandths of an inch offset from the true center of the tubing. Therefore two of the three longitudinal frame members had a slot that offset high and the third member offset low. As a result, the bolts for the main bearing carriers did not slide smoothly through the slot, thus larger holes were drilled to eliminate this interference with the slot.

The final difficulty that occurred during fabrication was keeping the rear shaft concentric through the rear bearings. Due to the natural warping affect that occurs during welding, welds across each of the three rear bearing carriers were staggered. The goal of staggering the welds was to cause natural pull in opposite directions to minimize the pull effects of the welds. Unfortunately, after completing the welds to mate the rear bearing carriers to the frame, the bearings were roughly 1 to 2 mm off center. This effect is not significant enough to impact the vehicle during testing, merely add minimal extra friction to the bearings. This, however; may result in measured power ratings that are lower than the true output power, ultimately reducing measurement accuracy.

RECOMMENDATIONS

After reviewing the completed design and fabrication, few recommendations could be made to further enhance the final project. The first and main concern lies within the fabricators ability to weld aluminum. Thus if the individual does not feel comfortable in doing so, he or she should avoid using aluminum for the frame because the tig welding process requires immense patience and persistence. The following concern involves the press fitting process of the bearings into the bearing carriers. The use of 5 thousandths of interference is too high for the bearings used in this application and should be reduced to no more than 3 thousandths. Additionally, caution should be taken while heating the bearing carrier to press the second bearings, due to the fact that the ball bearings may deform under high heat. This also applies to welding the pre-pressed rear bearing carriers to the frame, as the aluminum will quickly dissipate the heat to the bearings during the welding process. The final recommendation to the completed dynamometer consists of adding a tie rod unit to link the lower portions of the front bearing carriers to move as a single unit. The presence of multiple screws in a series of slots causes the bearing carriers to tip and tilt, result in inconvenience during adjustments.

REFERENCES

1. DTEC. 2002. Inertia Dyno Design Guide: Pakenham, Victoria, Australia: DTEC. Available at: http://dtec.net.au/Inertia%20Dyno%20Design%20Guide.htm. Accessed 18 February 2014.

2. EE. 2014. Dynamometer Review: Monroe, GA.: Engineer's Edge. Available at: http://www.engineersedge.com/industrial-equipment/dynamometer-review.htm. Accessed 18 February 2014.

3. Garcia, Jose, Janning, Lui, and Purvis. 2012. Supermileage Chassis Dynamometer. California Polytechnic State University Foundation.

4. L&SDCDS. 2014. Land & Sea's DYNOmite Chassis Dynamometer System: 20 January 2014. Concord, NH: Land & Sea. Available at: www.land-and-sea.com/chassis-dyno/chassis-dyno.htm. Accessed 12 February 2014.

5. McMaster Carr: Santa Fe Springs, CA.: McMaster-Carr. Available at: http://www.mcmaster.com/#8975kac/=s6njzv. Accessed 23 May 2014.

6. Sadhukhan, Debasis. 2013. Rotation. 21 July 2013. Allahabad, India: DEBASIS SADHUKHAN. Available at: http://www.hri.res.in/~debsadhukhan/HRI%20web/pdf/Rotation.pdf. Accessed 12 February 2014.

7. Zhao, Shupeng, and N. Ling. 2012. Chassis Dynamometer for Hybrid Electric Vehicle Based on Controller Area Network. In *Third International Conference on Intelligent Control and Information Processing.* Dalian, China: IEEEXplore.

APPENDICES

Appendix A: How Project Meets Requirements for the BRAE Major

Major Design Experience

Establishment of Objectives and Criteria
Project objectives and criteria are established to meet the needs of measuring and quantifying performance results of RC vehicles.

Synthesis and Analysis
The project will incorporate various stress calculations, as well as applicable kinematics for the system.

Construction, Testing and Evaluation
The dynamometer will be fabricated and tested to ensure operations and used to evaluate final vehicle performance.

Incorporation of Applicable Engineering Standards
The project will utilize AISC standards for allowable bending stresses and anticipated material deflections.

Capstone Design Experience

Incorporates knowledge/ skills from these key courses- BRAE 129 Lab Skills/Safety, BRAE 133 Engineering Graphics, BRAE 151 AutoCAD, BRAE 152 SolidWorks, BRAE 234 Mechanical Systems, BRAE 421/422 Equipment Engineering, Engineering Statics/Dynamics, Strength of Materials, Technical Writing

Physical- The device must be capable of testing various scale vehicles with varying wheel bases, combined with an adjustable restraint system.

Economic- The cost of the device will range $200-$300 in final cost.

Environmental- N/A

Sustainability- N/A

Manufacturability- The device will used standard dimensions and applicable working drawings for replication.

Health and Safety- The device will safely secure the vehicle during testing operations and contain unexpected projectiles during operation.

Ethical- N/A

Social- N/A

Political- N/A

Aesthetic- The completed device components will have machine finishes and the remaining aluminum will be polished to a respectable state.

Other – Productivity- The device will be capable of measuring and quantifying performance results of various RC vehicles.

Appendix B: Design Calculations

Mass Moment of Inertia Calculations

$$Volume = \left(\frac{\pi d^2}{4}\right) * l \quad (7)$$

Where,

π = 3.14
d = Diameter (m)
l = Length (m)

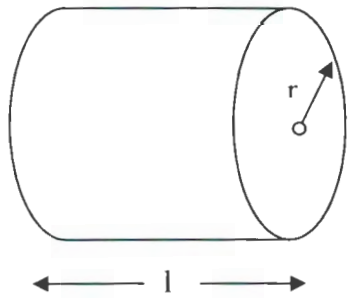

$$Volume = \left(\frac{\pi(.0635\ m)^2}{4}\right) * (.0762\ m) = .00024\ m^3$$

$$Mass = V * \rho \quad (8)$$

Where,

V = Volume (m^3)
ρ = Density of Steel (8050 kg/m^3)

$$Mass = (.0024\ m^3) * \left(8050\ \frac{kg}{m^3}\right) = 1.94\ \frac{kg}{roller}$$

$$I = \frac{1}{2}(m)(r^2) \quad (4)$$

Where,

I = Mass Moment of Inertia ($kg*m^2$)
m = Mass (kg)
r = Radius (m)

$$I = \frac{1}{2}\ (1.94\ kg * 2\ Rollers) * \left(\frac{.0635\ m}{2}\right)^2 = \mathbf{.0019\ kg * m^2}$$

TARGET MOI			SOLID (ON AXIS)		
Outer Radius Meters	Car Mass Kilograms	Target Roller MOI Kg.M^2	Outer Radius Meters	Roller Mass Kilograms	Solid Roller MOI Kg.M^2
0.0318	2.720	0.0027419	0.0318	3.8800	0.001955641
		0.0000000			0.000000000
		0.0000000			0.000000000
		0.0000000			0.000000000
		0.0000000			0.000000000
		0.0000000			0.000000000
		0.0000000			0.000000000
		0.0000000			0.000000000
		0.0000000			0.000000000
		0.0000000			0.000000000
		0.0000000			0.000000000
		0.0000000			0.000000000
		0.0000000			0.000000000
		0.0000000			0.000000000
		0.0000000			0.000000000
		0.0000000			0.000000000
		0.0000000			0.000000000
		0.0000000			0.000000000
TARGET MOI		0.002	SOLID TOTAL MOI		0.0019
TARGET MOI		(x10000)	0.002		

Frame Structural Calculations

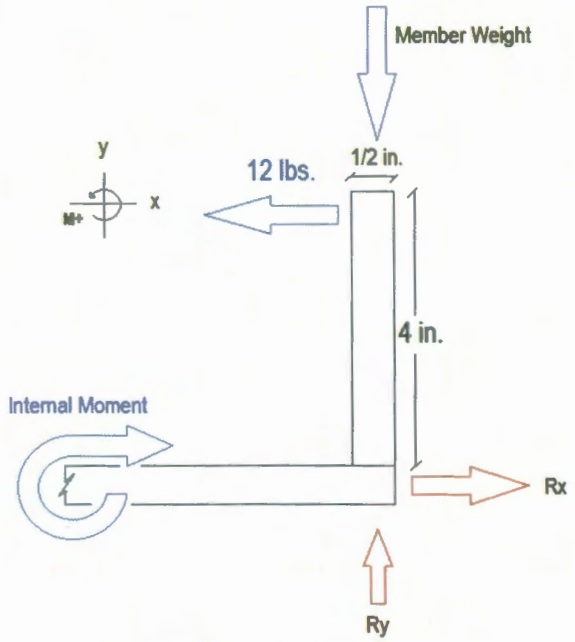

Retention Frame Free Body Diagram

$$\sigma = \frac{MC}{I} \tag{7}$$

Where,

σ = Stress (lb/in^2 or PSI)
M = Moment (in-lbs)
C = Distance to the Neutral Axis
I = Moment of Inertia

$$M = (12\ lb) * (4\ in) = 48\ in * lb$$

$$C = \frac{(\frac{1}{2}\ in)}{2} = \frac{1}{4}\ in$$

$$I = \frac{(\frac{1}{2}\ in) * (\frac{1}{2}\ in)^3}{12} - \frac{(\frac{3}{8}\ in) * (\frac{3}{8}\ in)^3}{12} = .0036\ in^4$$

$$\sigma = \frac{(48\ in*lb) * (\frac{1}{4}\ in)}{(.0036\ in^4)} = \mathbf{3{,}300\ PSI}$$

Alloy	Nominal Density (lbs./cu. in.)	Modulus of Elasticity, ksi x 10^3	Ultimate Tensile Strength, ksi	Elongation %	Melting Range, °F	Thermal Conductivity @ 77°F, unless otherwise stated (Btu/hr x in./sq. ft.)	Electrical Resistivity @ 68°F (Ohm-Cir. Mil/ft.)
1100, 1145, 1235	0.098	10.0	11-29.7	3-35	1190° to 1220°	1500-1600	16.8-18
2011	0.102	10.2	55-57	10-15	1005° to 1190°	1050-1060 @ 75° to 77°F	27
2017	0.101	10.5	62	22	955° to 1185°	930	31
2024	0.101	10.6	62-70	10-20	935° to 1180°	840 @ 75° to 77°F	30-35
3003, 3105	0.098	10.0	20-29	2-5	900° to 1210°	1100-1500	21-25
4032	0.097	11.4	55	8	990° to 1060°	960 @ 75°F	30
5005, 5205	0.098	10.0	20-26	4	1170° to 1210°	1390	20
5052	0.097	10.0	20-33	4-12	1125° to 1210°	960-1390	20-30
5083	0.096	10.3	44	12	1095° to 1180°	810	10.2
5086	0.096	10.3	40-47	10-12	1085° to 1185°	670	10.2-33
6013	0.098	10.1	55-65	5-11	1025° to 1205°	1140	Not rated
6020	0.098	Not rated	42-52	9-12	1080° to 1205°	Not rated	Not rated
6060	0.098	10.1	27.6-45	10-13	1030° to 1211°	1160-1449	19.25
6061	0.097-0.1	10.0	35-45	8-17	1080° to 1205°	1390 @ 75° to 77°F	24
6063	0.097	10.0	22-30	8-14	1110° to 1210°	1390-1452	15.8-28
6101	0.098	10.0	32	15	1080° to 1205°	96	24
7050	0.102	10.4	76	11	910° to 1165°	1090	25
7068	0.103	Not rated	103	9	Not rated	Not rated	Not rated
7075	0.101	10.4	71-83	9-13	890° to 1175°	900 @ 75° to 77°F	31
MIC6	0.101	10.3x10^6	24	3	1200°	984	Not rated
Porous Mold-Quality	0.065	1.3	Not rated	Not rated	Not rated	Not rated	Not rated
QC-10	0.103	10.4	82	10	1050°	1104	Not rated

$$Factor\ of\ Safety = \frac{Material\ Strength}{Design\ Load} \tag{8}$$

Where,

Material Strength = 20-30 ksi

Design Load = 3.3 ksi

$$F.S. = \frac{20\ ksi}{3.3\ ksi} = \mathbf{6.0}$$

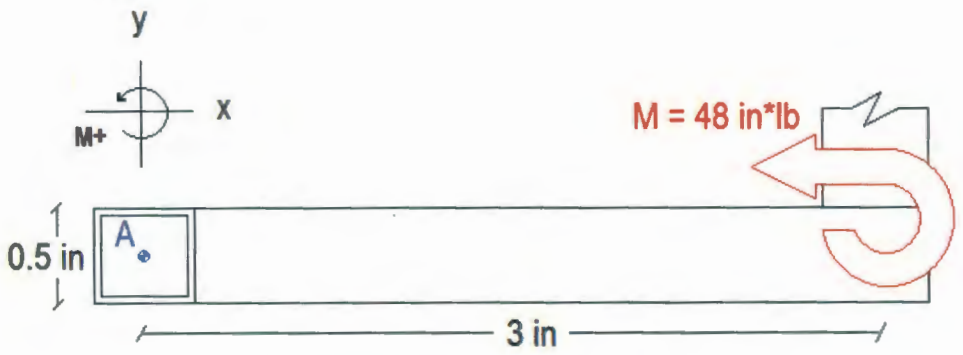

Lower Retention Frame Free Body Diagram

$$\theta_{MAX} = \theta(L) = \frac{ML}{EI} \tag{9}$$

Where,

θ_{MAX} = Maximum Angular Deflection

L = Length (inches)

E = Young's Modulus = 102,000 ksi (5052 Aluminum)

I = Moment of Inertia

$$\theta_{MAX} = \frac{(48\ in * lb)(4\ in)}{(102{,}000\ ksi)(0.0036 in^4)} = \mathbf{0.225\ degrees}$$

Appendix C: Stage 2 Dynamometer Working Drawings

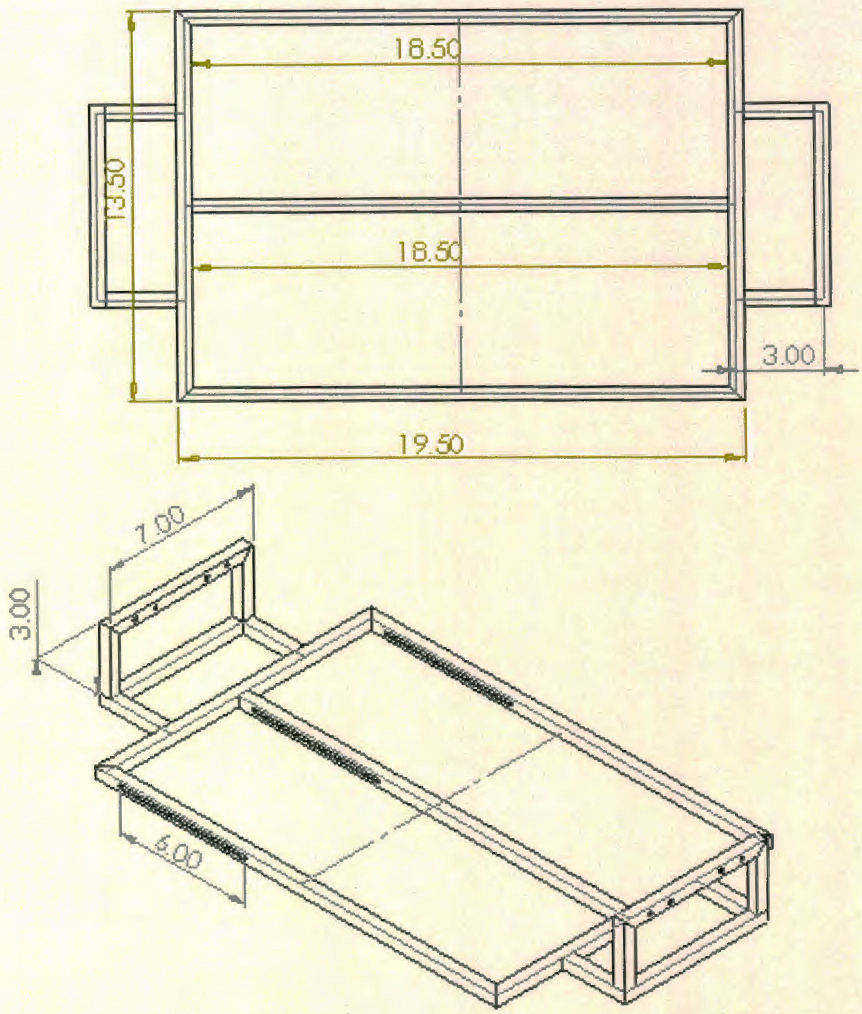

Note: Mill slotted section prior to welding

Aluminum

Main Frame DRAWING

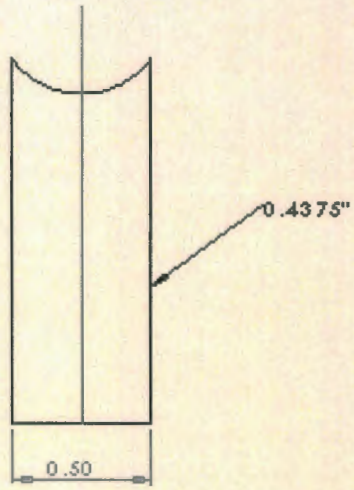

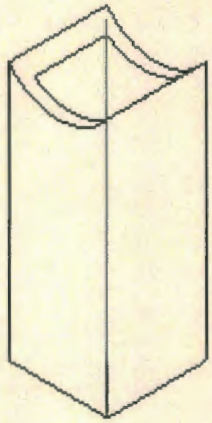

Note: Potential Saddle required

Aluminum

Bearing Vertical DRAWING

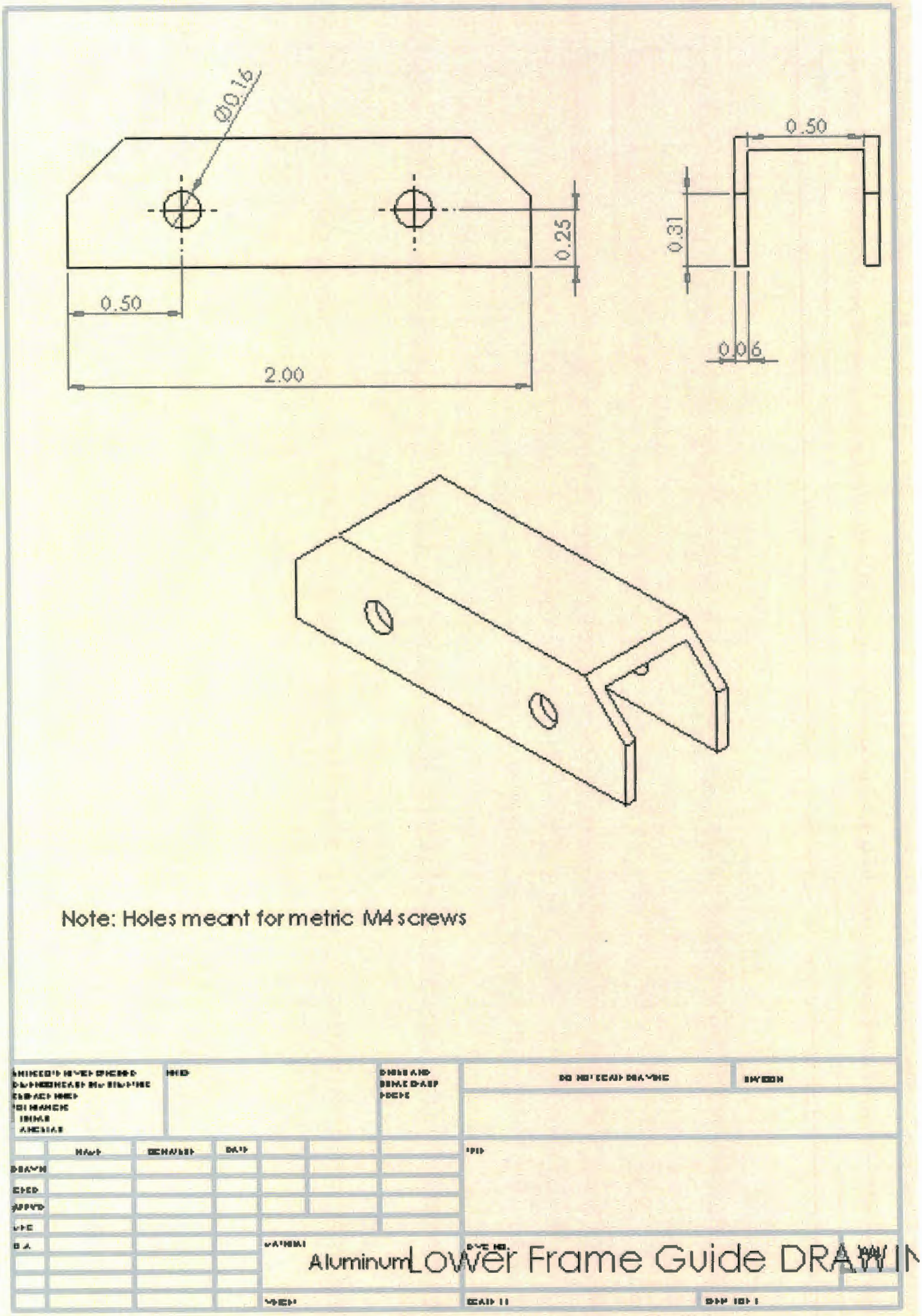
Ø0.16
0.50
0.25
0.31
0.50
0.06
2.00
Note: Holes meant for metric M4 screws
DO NOT SCALE DRAWING
Aluminum
Lower Frame Guide DRAWIN

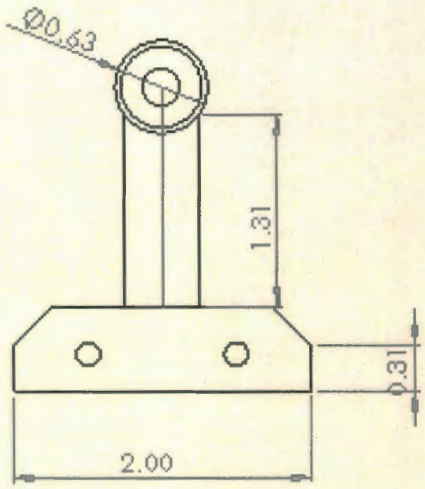

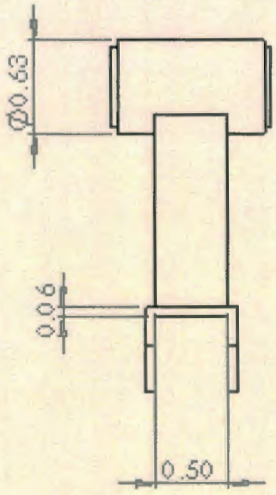

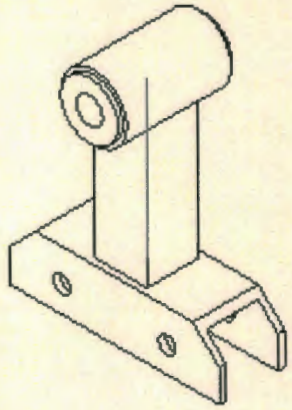

Note: Potential saddle required

Standing Bearing Assembly DRA

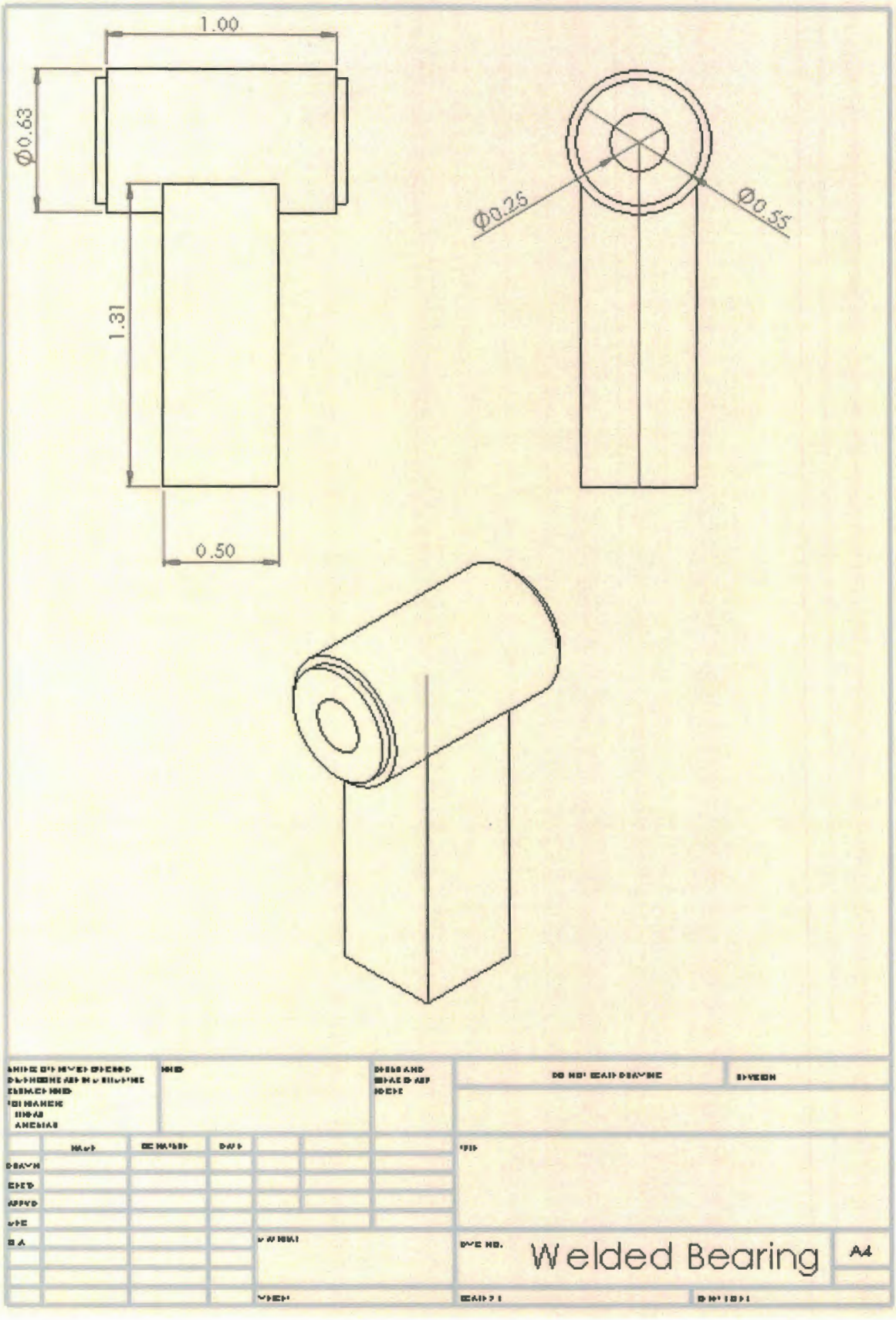
1.00
Ø0.63
1.31
0.50
Ø0.25
Ø0.55
Welded Bearing
A4

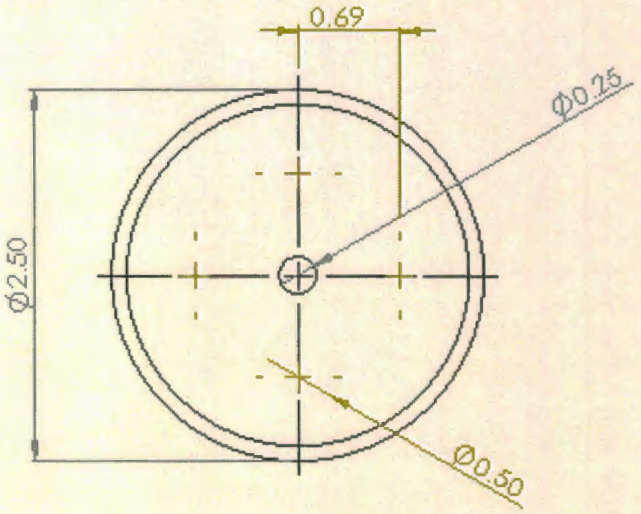

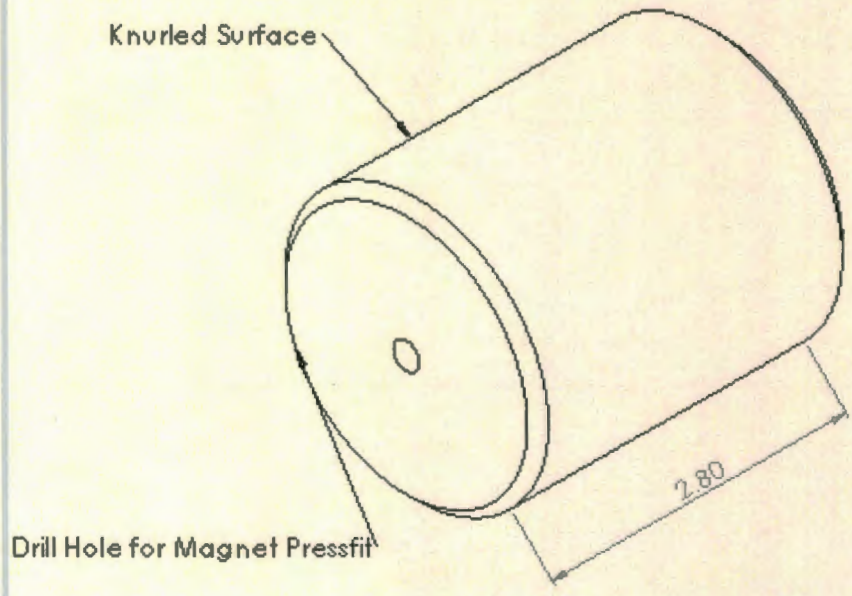

Steel

Prime Roller DRAWING

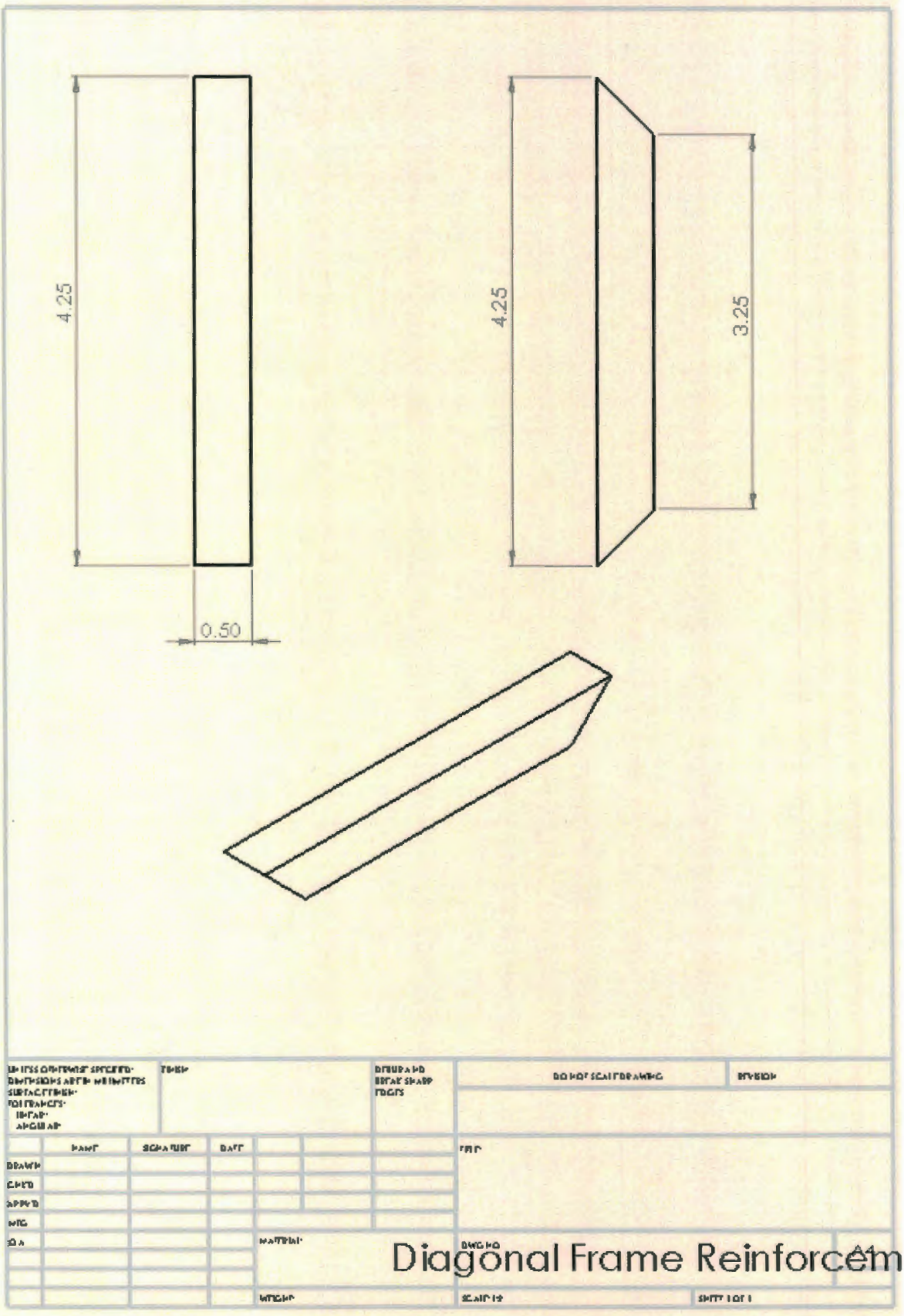
4.25
0.50
4.25
3.25
Diagonal Frame Reinforcem

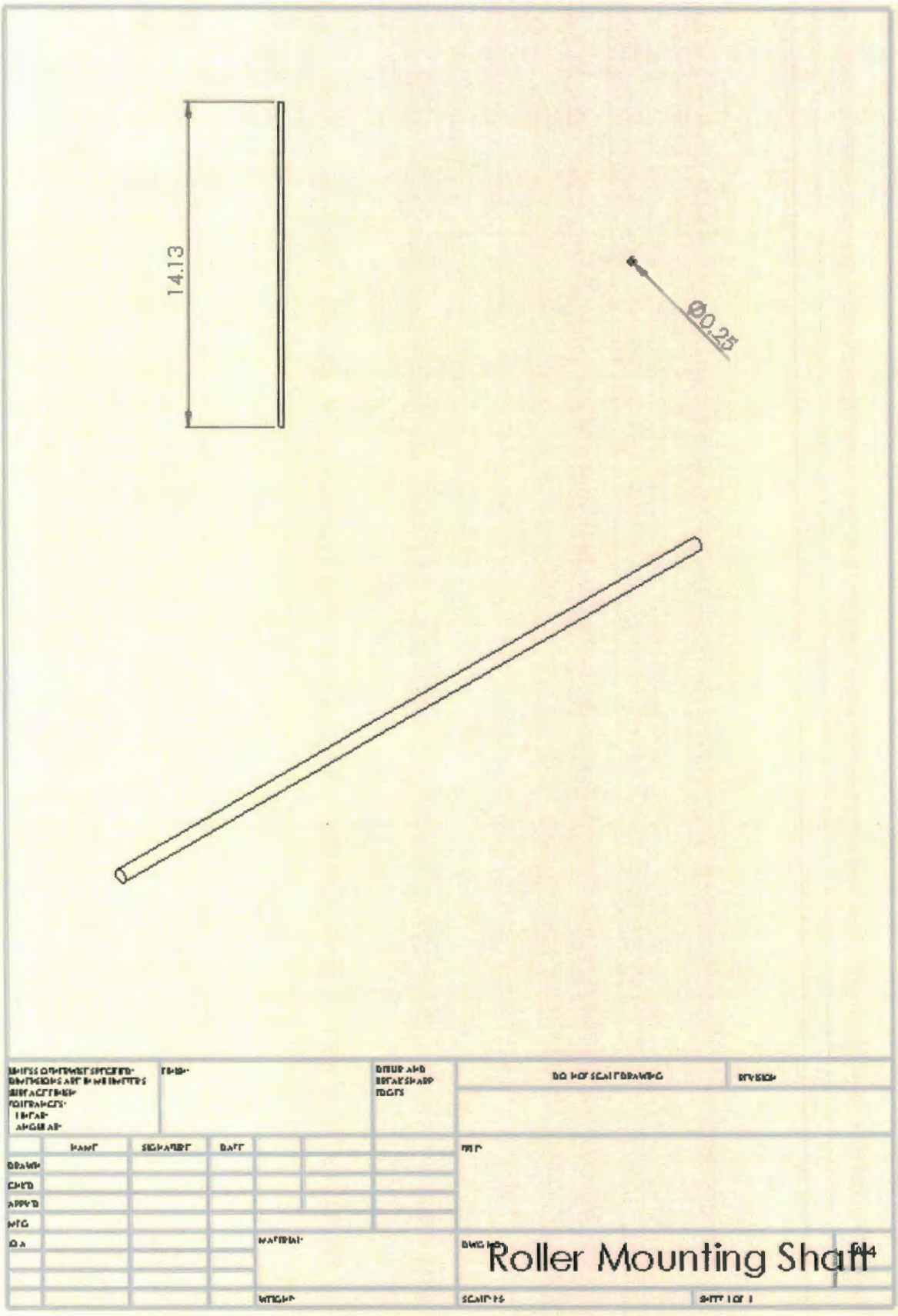
14.13
Ø0.25
Roller Mounting Shaft

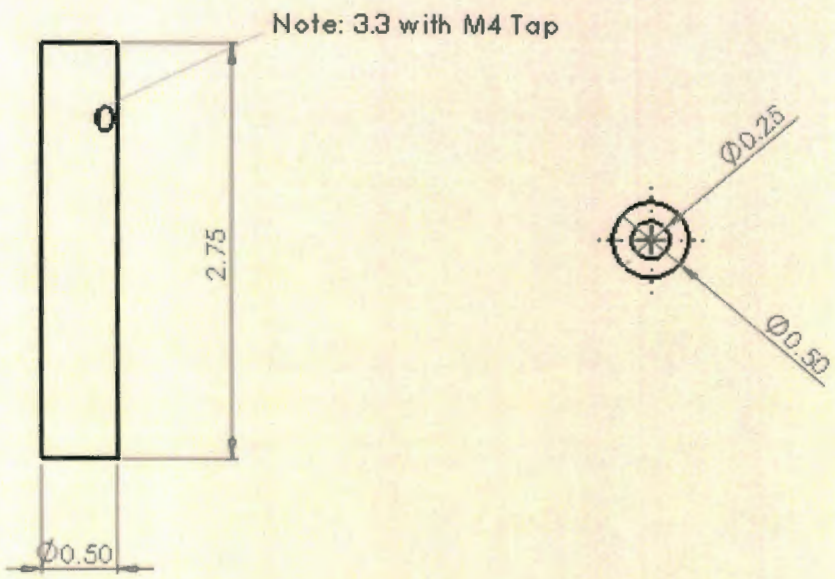

UNITS OF MEASURE SPECIFIED: DIMENSIONS ARE IN MILLIMETERS SURFACE FINISH: TOLERANCES: LINEAR ANGULAR:		FINISH:				BREAK AND BREAK SHARP TO 0.25	DO NOT SCALE DRAWING	REVISION
	NAME	SIGNATURE	DATE				TITLE:	
DRAWN								
CHK'D								
APPV'D								
MFG								
Q.A				MATERIAL:			DWG NO. Telescope Center	A4
				WEIGHT:			SCALE:1:1	SHEET 1 OF 1

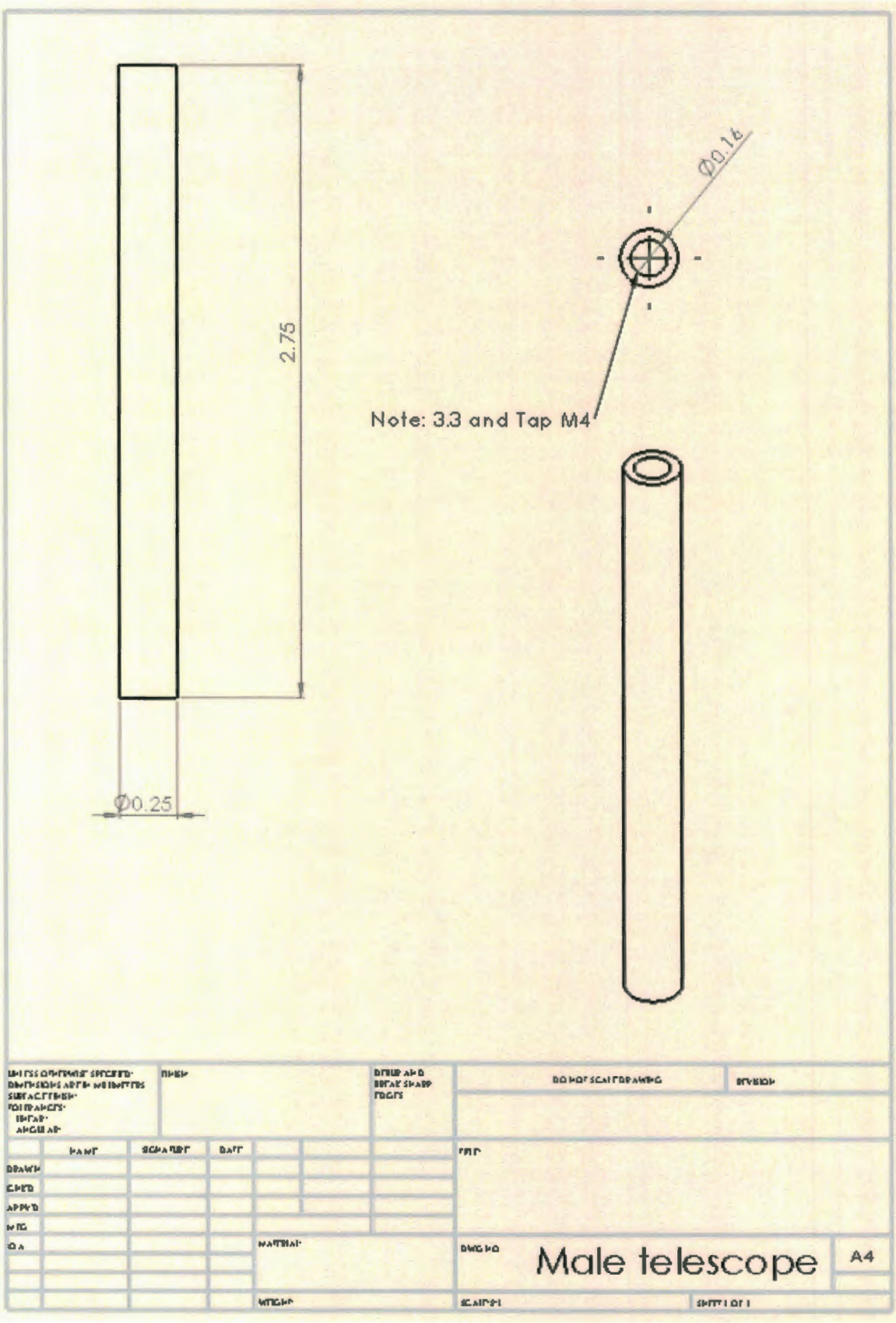
2.75
Ø0.25
Ø0.18
Note: 3.3 and Tap M4
Male telescope
A4

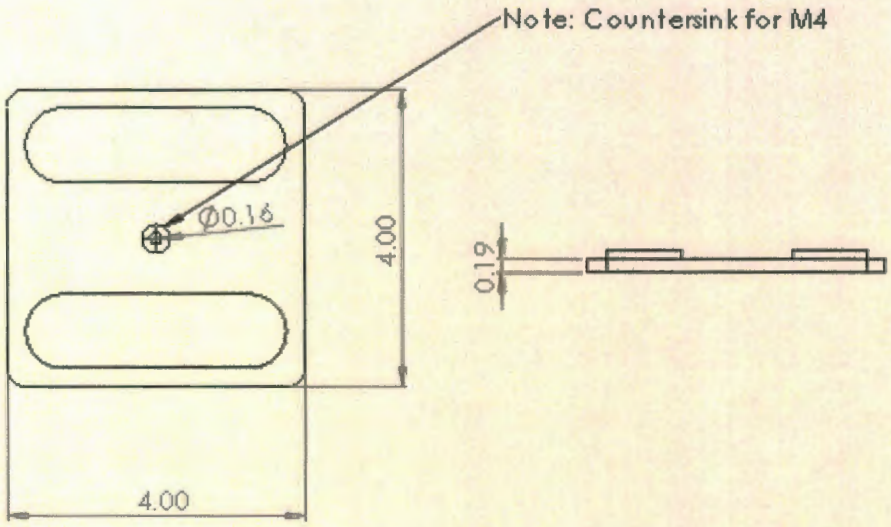

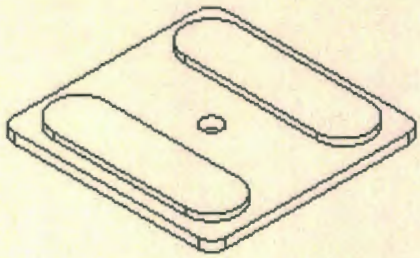

Stabilization Platform

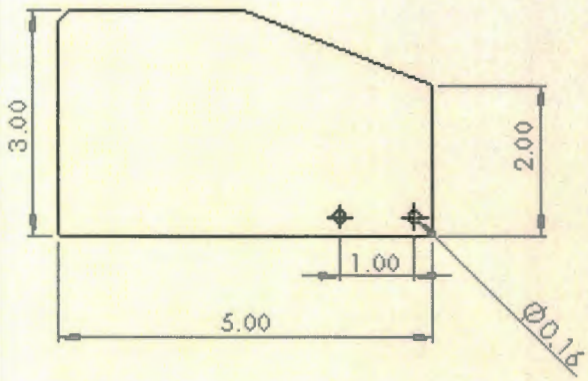

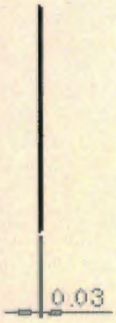

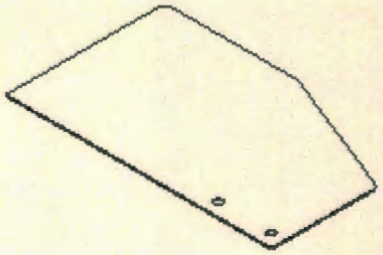

carbon fiber guards